Dynamic optimization of emergency resource scheduling in a large-scale maritime oil spill accident

Abstract: Current maritime emergency logistics studies on oil spills are largely conducted based on static analysis to optimize resource scheduling. This does not suitably address the practical industrial demand, where the oil spill risk in nature dynamically depends on the motion of oil films. To better simulate the reality, this paper aims to conduct a study on a novel dynamic multi-objective location-routing model with split delivery considering practical characteristics, such as the time-varying demands of contaminated areas, uncertainty in the state of associated transportation networks and interrelationship between the changes in spilled oil films and emergency operations, which all result from the dynamic motion of oil films at sea. To address model complexity, we propose a two-stage optimization model, whereby a hybrid heuristic algorithm is developed to obtain Pareto solutions. To demonstrate the proposed model and approaches, a case study involving a series of sensitivity analyses is presented to highlight the importance of the proposed model and determines its implications.

Key words: Emergency logistics; Maritime oil spill; Split delivery; Location-routing problem; Hybrid heuristic algorithm

1 Introduction

Offshore oil exploration and tanker vessels are the major sources of accidental oil spills in the marine environment (ITOPF, 2020). With the rapid development of offshore oil exploration and transportation activities at sea, the risk of major maritime oil spill accidents is increasing year by year (Garrett et al., 2017). When a large-scale maritime oil spill occurs, the decision making for the emergency response can be challenging and intractable. This is because decision makers (emergency and rescue commanders) must coordinate numerous resources and develop appropriate response schemes with considerations of urgency (Xu et al., 2016), uncertainty (Huang et al., 2020), resource constrains (Liu et al., 2018) and potential consequences (Wang et al., 2020).

For example, BP's oilfield in the Gulf of Mexico experienced a serious spill in 2010, which caused great damage to the ecological environment of the coastal areas, with an estimated cost of more than $20 billion. After the Deepwater Horizon Oil Spill occurred, under the charge of the U.S. National Commission on the Deepwater Horizon Oil Spill and Offshore Drilling, over 39,000 personnel, 5000 vessels and 110 aircrafts were dispatched, over 700 km booms were deployed, 275 controlled burns were carried out, approximately 27 million gallons of oil-water mixture were recycled by skimmers, and more than 1.5 million gallons of dispersant were used. Nevertheless, improper decisions on emergency resource scheduling usually caused waste to manpower and budgets (U.S. National Commission on the Deepwater Horizon Oil Spill and Offshore Drilling, 2011). It is followed by another large-scale oil spill of ConocoPhillips in the Bohai Bay in 2011, which polluted an area of about 6,200 square kilometers around and northwest of the oilfield and 870 square kilometers of which was heavily polluted. Compared with the national oil spill emergency response system in the U.S., China's

oil spill emergency response system was still in its infancy stage and had not yet formed a complete emergency response mechanism (He, et al., 2013). Therefore, there were a lot of deficiencies in department coordination and emergency resource scheduling. After interviewing the local maritime bureau that was directly involved in the emergency response, we have learned that the vessels participating in the emergency response composed of the local maritime department's own emergency vessels and private vessels of the surrounding ports and fishermen. Nevertheless, the emergency operations and transportation activities of these vessels in the emergency response were completely autonomous and lack of overall planning, which leaded to the low efficiency of the emergency response. More recently, in 2018, the Panamanian-flagged tanker Sanchi that was carrying 110,000 tons of condensate oil collided, collided with the Hong Kong-flagged cargo ship CF Crystal in the East China Sea. About 1,900 tons of the Sanchi's own fuel oil and unknown amount of condensate sank along with the Sanchi. Under the command of the Ministry of Transport in China, various regional/provincial administrations such as the East China Sea Rescue Bureau and the Shanghai Salvage Bureau were mobilized to clean up the spilled oil. The total area of cleanup was up to 225.8 square nautical miles. Compared with the oil spill emergency response in the Bohai Bay in 2011, China's oil spill emergency response mechanism was considerably improved and the emergency force carried out emergency operations and emergency resource transportation in the form of marshalling, which improved the responsiveness to some extent. However, there was only a macro division of the responsibilities of the relevant emergency forces without specific instructions for emergency operations and means of resource coordination among them (Yin, 2019).

Thus, it can be seen that a large-scale oil spill may occur anywhere at any time, which has always represented a major threat to human society. However, in terms of the actual state of the emergency response to oil spills, decision makers more or less face the problem of the uncoordinated scheduling of emergency resources. Several officials from the Maritime Safety Administration of China who have participated in the response efforts to the ConocoPhillips oil spill in the Bohai Bay admitted that due to the absence of theoretical decision support, the scheduling of oil spill emergency resources usually relies on subjective experience, which can result in a low responsiveness and even chaos in the emergency response. A severe oil spill emergency situation requires us to conduct the research on emergency resource scheduling to enhance the practical emergency efforts in response to oil spills. Of course, a series of catastrophic oil spills has created a shockwave globally across the industry, government, and research community (Ye et al., 2019). Subsequently, the problems related to oil spill emergency have become the research area of increased interest, which has resulted in a large number of studies on contingency management, environmental impact assessment, and simulation technique development (Payam et al., 2019; Xiong et al., 2015; Wang et al., 2020; Chen et al., 2016). Nevertheless, there are only a limited number of studies on the development of process optimization and decision making in maritime emergency logistics targeting oil spills. Research on the scheduling of emergency resources in response to oil spills remains in the early stage.

In contrast to the studies on maritime emergency logistics, the problems of

emergency resource scheduling in regard to land-based disasters have been extensively studied in recent decades and notable progress has been attained in research on land-based emergency logistics (Alem et al., 2016). The context of emergency operations after large-scale land-based disasters can be dynamic and challenging. The demand for emergency resources in affected areas may change over the phase of the response efforts depending on conditions, such as livelihood recovery and secondary disasters (Campbell et al., 2018). Similarly, the state of transportation networks can also vary due to any road damage caused by disasters and transportation recovery (Mehmet et al., 2020). Such characteristics of land-based emergency logistics highlight that any developed models must fully consider the changing conditions in the emergency response to effectively support decision makers. Therefore, a great deal of research on land-based emergency logistics has been devoted to address the dynamic issues in the emergency response, and a series of theoretical approaches has been developed to reflect the dynamic decision-making environment (Abdolhamid et al, 2020; Maharjan et al., 2020; Cao et al., 2018; Alem et al., 2016). Although numerous empirical research results have demonstrated that these approaches have good application effect in the process of making decisions on land-based emergency logistics, their assumptions are too restrictive to be applicable to making decisions on maritime emergency logistics. In response to land-based disasters, the changing conditions exhibit periodic persistence characteristics. Each time external conditions change, the resulting state lasts for a period of time. Frequently used approaches have been developed based on these characteristics and are naturally applicable to the emergency response to land-based disasters. In contrast, the dynamic characteristics of the emergency response to oil spills mostly depend on the dynamic motion of oil films (i.e., diffusion and drift). Diffusion could lead to an increase in the size of the contaminated area to be cleaned up, resulting in a change in the demand for emergency services. Moreover, drift could alter the position of oil films and consequently affect the transportation routes of the vessels participating in the response. The dynamic motion of oil films is continuous in reality, which implies that the external conditions in the response to oil spills also continuously changing over time. Within the content of the maritime decision-making environment, the assumptions of the above frequently adopted approaches to land-based emergency logistics are obviously inapplicable, that the state of external conditions can be maintained constant for some time before subsequent changes occur. To simplify the problem of maritime emergency logistics, the reviewed studies on emergency resource scheduling in response to oil spills have usually neglected the characteristics of the dynamic motion of oil films, which could be the reason why decision makers are reluctant to apply the existing analytic models and may explain the absence of effective theoretical support for decision making. From this point of view, it is of great significance to develop a novel methodology based on the characteristics of the oil spill emergency response to bridge the above research gap and to provide theoretical support for decision makers in terms of emergency resource scheduling to cope with oil spills at sea.

To be specific, the emergency response to major oil spills represents a complicated decision-making problem and the response strategy has usually relied on methods such

as mechanical, chemical and biological techniques (Li et al., 2016). Mechanical techniques are recognized as the most environmentally friendly solutions, as they all directly remove pollution from the sea. Therefore, mechanical recovery (i.e., skimming) belonging to mechanical techniques tends to be one of the most preferred options despite the corresponding high capital investment and operational complexity (Li et al., 2014b; Wang et al., 2018). In the emergency response to major oil spills, mechanical recovery usually plays a vital role in spilled oil cleanup tasks. Besides, mechanical recovery requires support from vessels and trained personnel which can be highly affected by harsh conditions due to the dynamic motion of the oil films and the fragile marine ecosystems (Li et al, 2014b). It is desirable to conduct oil spill recoveries under such conditions in a timely manner. Keeping this in mind, we realize the necessity and significance of developing an effective emergency resource scheduling methodology for oil spill emergency response, especially mechanical recovery. Moreover, when a large-scale oil spill occurs, the available resources (both monetary and non-monetary) are often considered to be economically constrained (Huang et al., 2020; Xu et al., 2016). Decision makers therefore have to ensure a high responsiveness while balancing the economic cost and effect. Therefore, we are determined to propose a novel optimization model to provide decision makers with an efficient emergency resource scheduling strategy for recycling spilled oil via mechanical recovery by striking the balance between responsiveness and the total response cost. We consider the changing conditions in the maritime decision-making environment by developing a time-varying planning approach, which enables decision makers to consider the time-varying demand of emergency services and the uncertain state of transportation networks caused by the dynamic motion of oil films.

The remainder of this paper is organized as follows. Section 2 provides the literature review about emergency logistics problems related to our work. Section 3 briefly reviews the problem definition and analyzes the dynamic motion of oil films, which provides the foundation for the model formulations. Section 4 develops the model for optimal scheduling of emergency resources in the response to a large-scale maritime oil spill. Section 5 proposes a hybrid heuristic algorithm to deal with the model and adopt an alternative quantitative method to select the optimal option from the set of Pareto non-dominated solutions. Next, the model and algorithm are applied in a case study and a series of scenarios are depicted to test the performance of the model and the proposed approaches in Section 6. Finally conclusions are drawn in Section 7.

2 Literature review

Decision makers always face intractable challenges in developing efficient emergency resource scheduling schemes due to the existence of various uncertainties (Wang et al., 2014). For instance, with burstiness of disaster events, decision makers are often unable to gather data in advance on affected areas so that they must make decisions in the face of uncertain demand. Moreover, demand in emergency resources could change over the course of emergency response due to changes in external conditions. So does the infrastructure status (transportation networks). To solve the issues of uncertainty and dynamics in the crucial emergency period of a large-scale

land-based disaster, the following three approaches have been widely adopted: the time period planning horizon (e.g., Abdolhamid et al, 2020; Loree et al., 2018; Maharjan et al., 2020; Zhou et al., 2017), the rolling planning horizon (e.g., Daniel et al, 2020; Liu et al., 2019; Lu et al, 2016; Huang et al., 2015; Cao et al., 2018) and the scenario planning approach (e.g., Zhang et al., 2019; Gökalp et al, 2020; Hu et al., 2019; Ahmadi et al., 2015; Alem et al., 2016). The time period planning horizon approach describes the response phase into several fixed time periods so that the complicated dynamic problem is transformed into a relatively static problem to address easier (Hoyos et al., 2015). In the rolling planning horizon approach, multiple planning horizons are considered and the parameters of the model can be updated at the beginning of each horizon. According to Huang et al. (2015), it is able to effectively address the uncertainties in disaster response because decisions can be revised at several time points based on the available real-time information. The scenario planning approach is proposed on the basis of disaster scenario information updates in an attempt to coordinate efficiency and cost through timely and appropriate decisions regarding issues such as vehicle routing and emergency resource allocation. Scenario analysis largely targets long-term decision making and strategic planning (Charles et al. 2016; Ransikarbum et al, 2016). Although this approach is obviously superior to a deterministic approach which ignores the uncertainty presented in practice, it is often not very efficient for coping with real-world problems (Najafi et al., 2013).

Emergency logistics has received increased attention in the reviewed literature, but most of the existing studies have focused on the emergency response to land-based disasters (Alem et al., 2016). Even under the context of the land-based decision-making environment, the emergency resource scheduling strategy encompasses rather difficult tasks to be accomplished. These difficult situations may become even more sophisticated and worse when the decision making becomes more dynamic depending on the uncertainty of changing maritime conditions. As a result, the aforementioned approaches can effectively copy with dynamic issues existing in the emergency response to land-based disasters, but they are not qualified to deal with the dynamic emergency response to oil spills at sea. This is mainly due to the essential differences between the land-based and maritime decision-making environments. In regard to uncertainty, the main assumptions of the commonly adopted approaches (e.g., the time period planning horizon and the rolling planning horizon) to the existing emergency logistics models are that the demand for emergency resources and transportation network state in the affected areas remain relatively stable at different time intervals. Only when the emergency response phase reaches several specific time points will the demand and transportation network state in the system be updated. In the emergency response to maritime oil spills, these assumptions are too restrictive and are thus inapplicable. Under the action of surface tension, oil films at sea continuously diffuse, resulting in the continuous expansion of the contaminated areas. Since the demands of contaminated points for oil spill cleanup services are usually positively correlated with the oil film areas, the demands correspondingly increase with increasing oil film diffusion. In addition, oil films may simultaneously drift under the influence of waves and currents, which indicates that the transportation routes of vessels may change

dynamically as a result. The aforementioned dynamic processes occur constantly, without pauses or periodic changes. Herein, we should apply the time-varying approach representing the dynamic conditions in the response to oil spills instead of the conventional approaches proposed for the response to land-based disasters.

Moreover, the existing studies have focused on only the impact of the uncertainty in external surroundings on emergency logistics (Abdolhamid et al., 2020; Zhang et al., 2019; Daniel et al., 2020; Loree et al., 2018; Maharjan et al., 2020;). Few studies have addressed the influence of emergency operations on both the demand for emergency services and state of transportation networks. In fact, because oil films have dynamic motion in terms of diffusion and drift, there exists an interrelationship between the changes in oil films and emergency operations regarding emergency resource scheduling. On one hand, there is no doubt that the changes in the area and position of oil films affect the scheduling decision. On the other hand, emergency operations impact the changes in oil films as well. For example, the efficient scheduling of vessels equipped with skimmers can clean up the oil film and reduce the quantity of the spilled oil in a timely manner, thus effectively restraining the diffusion of the oil film, which is closely related to the spilled oil quantity. It could be more justified when there is no existence of emergency logistics models capable of addressing the particular concern of increasing size of oil tankers leading to larger-scale oil spills, which requires the time-varying model considering interrelationship between the changes in the decision-making environment due to dynamic motion of the oil films and emergency operations. Therefore, how to quantitatively analyze the interrelationship between emergency resource scheduling and changes in the oil films, which is usually ignored in the literature reviewed, is a vital and urgent task in the field.

In addition, given the high demand for emergency resources in the affected areas during the emergency response phase, decision makers inevitably need to resolve the issue of an insufficient transportation capacity. In this case, they need to consider the available transportation serving an affected area several times instead of the one-time delivery proposed in most emergency logistics models. This phenomenon is referred to as split delivery in the relevant studies (Hu et al., 2019; Daniel et al., 2020; Liu et al., 2019; Moreno et al., 2018; Wang et al., 2014; Lin et al., 2011). Dror and Trudeau (1989) first empirically showed that benefits could be obtained by adopting split delivery in both the total travel distance and number of vehicles required to deal with the limited transportation capacity. However, the existing models considering split delivery only require emergency resources to be delivered before the end of the emergency response phase and do not consider the specific consumption process in detail, which is sufficient to deal with land-based emergency logistics but is unable to meet the requirements of oil spill emergency response. In the land-based emergency response, sufficient emergency resources can ensure responsiveness as long as they are delivered within the required time limit, and redundant resources that are not currently needed can be stored at the demand points for subsequent use. In contrast, in the absence of storage conditions at sea, the transportation of emergency resources must be coordinated with the specific cleanup operations (i.e., the consumption of emergency resources). Since the loading capacity of an emergency vessel is limited and no storage conditions are

available at sea, immediate replenishment is necessary before the emergency resources of the emergency vessel are depleted.

At present, there are only a limited number of studies on the emergency response to chemical spills at sea (Grubesic et al., 2019; Garrett et al., 2017; Huang et al., 2020; Xu et al., 2016; Liu et al., 2018; Li et al., 2014a). To our knowledge, these studies do not fully consider the essential characteristics of the emergency response to chemical spills at sea. To ensure the effectiveness of the proposed emergency resource scheduling strategy in practice, we take advantage of the fact that it can be adequately represented by mathematical models of the oil film dynamic motion whereby oil films continue to diffuse and drift at sea (Chen et al., 2016). Consequently, both the demands in the contaminated areas and the state of transportation networks at sea are to be addressed through the time-varying planning approach, which makes use of time-varying parameters and constraints to reflect the dynamic conditions in the emergency response and provides a foundation to address the interrelationship between emergency operations and oil film changes. When considering split delivery, we also set a corresponding time window based on the characteristics of the emergency response to maritime oil spills to ensure that the delivery of supplementary emergency resources is completely consistent with the actual cleanup operations. Ultimately, this paper proposes, in nature, a dynamic multi-objective location-routing model to determine the emergency resource reserved bases (ERRBs) to constitute those fleets participating in the emergency response and to manage the routes of the fleets dispatched to clean up the spilled oil and transport supplementary resources.

To support the trade-offs between the responsiveness and total response cost, the proposed model has two objective functions: minimization of the value of the ecological loss caused by oil spill pollution, and minimization of the total response cost. However, there are always contradictions between the various objectives in a multi-objective optimization problem. Therefore, it is difficult to determine a unique non-dominated solution satisfying all the optimization objectives. Generally, multi-objective problems are resolved using the weighted sum method (Baharmand et al., 2020; Maharjan et al., 2020; Cao et al., 2018; Oscar et al., 2018; Huang et al., 2015; Ransikarbum et al., 2014). The main idea is to assign a certain weight to each objective and convert the multi-objective problem into a single-objective problem. Nevertheless, the quality of the solution obtained heavily depends on the assigned weight coefficient, and weight setting often occurs too subjectively and unreasonably (Zhang et al., 2019). Therefore, we adopt an alternative solution based on the cost performance method to determine the ideal option from the obtained non-dominated solutions, which effectively avoids the subjectivity of the weight coefficient setting and ensure the validity and rationality of the selected solutions.

The main contributions of this paper include:

1 This paper develops the time-varying approach to present the dynamic conditions in the emergency response to oil spills instead of utilizing conventional approaches proposed for land-based emergency logistics, which are not applicable to supporting the decision making in the maritime environment.

2 The interrelationship between the decision-making environment and emergency

operations is taken into consideration in a pioneering way, which is vital to the emergency response to oil spills but is always neglected in the existing literature.

3 To solve the issues of insufficient transportation capacity in the oil spill emergency response, an optimization model with split delivery is developed. Considering that the storage conditions in the maritime environment and the land-based environment are essentially different, this paper make use of the corresponding time window for split delivery to coordinate emergency operations and transportation of supplementary emergency resources for oil spills, which is hardly considered in the land-based emergency logistics but is necessary for the emergency response to oil spills.

4 An alternative solution based on the cost performance method is adopted to select the ideal option from the obtained non-dominated solutions for the proposed multi-objective model.

3 Background of the problem

Here, we describe the problem of scheduling emergency resources for oil spills. This paper aims to respond to a major oil spill accident by means of transporting and delivering emergency resources to the demand points at sea. However, the dynamic motion of oil films always plays an important role in the response to oil spills. Hence, the dynamic motion of oil films is also analyzed in this section.

3.1 Problem definition

The emergency response to maritime oil spills is sophisticated and the framework requires support from numerous methods. Since mechanical recovery (i.e., skimming) is the most common means of cleaning up spilled oil (Li et al., 2014b; Wang et al., 2018), this paper focuses on the emergency resource scheduling required for mechanical recovery. To be specific, mechanical recovery utilizes the vessels equipped with skimmers (i.e., emergency vessels) to recycle spilled oil mixed with seawater. The recycled oil-water mixture is then loaded into onboard floating oil bladders to clean up the contaminated area. Due to the limited capacity of the floating oil bladders onboard the vessel, the emergency response faces the problem of the insufficient capacity of the emergency vessels. In a real-world oil spill emergency response, to address these issues, another type of vessels (i.e., transportation vessels) must be implemented to provide emergency vessels with a continuous supply of empty floating oil bladders to ensure that the emergency work is continuously executed. The fully-loaded floating oil bladders are transported by the transportation vessels to the ERRBs or surrounding ports for emptying. Different emergency fleets are responsible for various demand points, and the number of times they need to retrieve supplies is also various, which requires the transportation fleet to complete supply transport via split delivery.

It is worth noting that the emergency response to large-scale oil spills is often associated with a centralized decision-making organization. The organization is under the command of the administrative department at the national/reginal level to schedule emergency resources and to assign tasks during emergency operations to related participants and emergency forces. This was evident from the emergency responses to the Deepwater Horizon Oil Spill in the Gulf of Mexico and the Sanchi incident in China. When decision makers formulate a corresponding scheduling decision, the first aspect to be considered involves the dynamic changes in oil films at sea. This process mainly includes diffusion and drift, which implies that the area and position of oil films continuously expand and change over time. Since the workload of emergency operations and the consumption of emergency resources are often proportional to the

oil film area, the demand for emergency services and resources at each demand point also varies over time during the emergency response. Similarly, when emergency resources are transported to each demand point, the transportation networks also exhibit time-varying features to oil film drift.

To demonstrate the decision-making process, an illustration is shown in Fig. 1. First, efficient cleanup of the spilled oil in a timely manner with emergency fleets inhibits the expansion of oil films to reduce the contaminated area and time to recover the spilled oil. The recycled oil-water mixture volume and the cleaning area of the skimmers remain fixed per unit time. If a longer emergency response is needed, this means that the emergency fleets require more emergency resources (i.e., oil floating bladders) to handle the recycled oil-water mixture, which increased in volume. Furthermore, when analyzing the relationship between the travel distance and emergency operations, the situation becomes more complicated. If oil films drift toward the ERRBs, the later the emergency fleet arrive at the demand points, the shorter the travel distance will be, and vice versa. In contrast, if oil films drift away from the ERRB, the earlier the emergency resources arrive at the demand points, the shorter the travel distance will be, and vice versa. When the floating oil bladder capacity of the emergency fleet is insufficient, it is necessary to make a corresponding decision on transport of supplementary resources to ensure that additional floating oil bladders reach the position of the emergency fleet before the capacity is exhausted. In contrast to conventional land-based emergency resource scheduling, the potential impact of emergency operations on oil film changes must be considered in the decision-making process of emergency resource scheduling in response to large-scale maritime oil spills in addition to the impact of oil film changes on scheduling decisions.

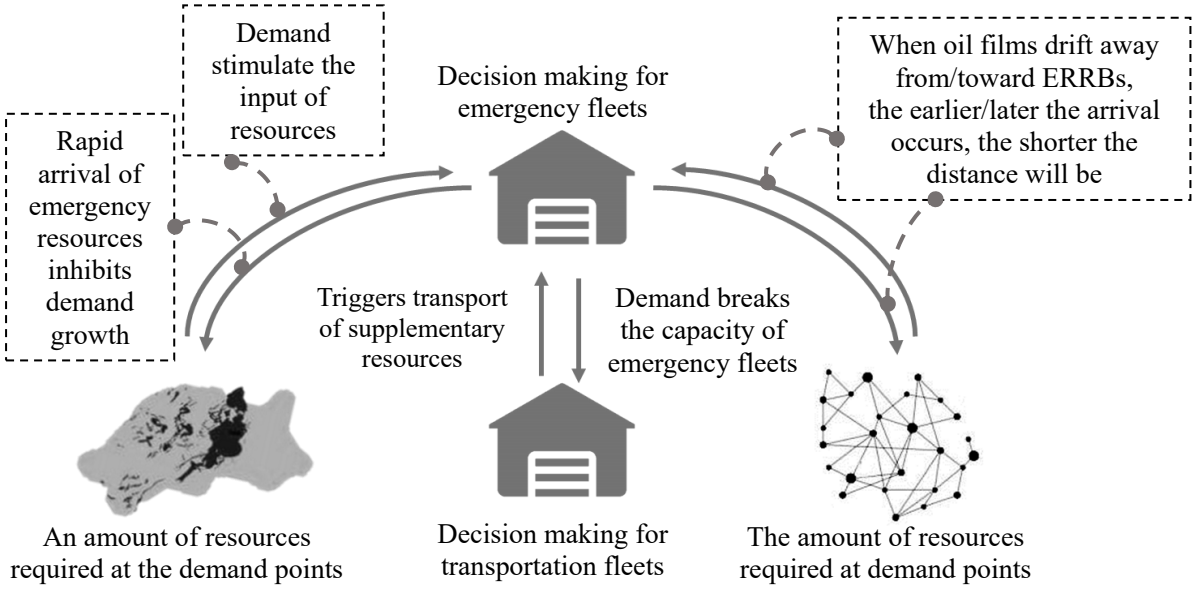

Fig. 1. The flow chart of the decision-making.

This paper aims to help the centralized decision-making body to coordinate the emergency response and delivery of emergency resources from the ERRBs to the demand points. The specific actions required in a scheduling scheme are: 1) to determine the ERRBs to provide the emergency fleets; 2) to plan the routes for the emergency fleets; and 3) to dispatch vessels to the emergency fleets. Once the demands of any contaminated area break the capacity of the emergency fleets, we also need to decide how 4) to determine the ERRBs to provide the transportation fleets; 5) to plan

the routes for the transportation fleets to provide supplementary floating oil bladders for the emergency fleets facing a shortage in the capacity of floating oil bladders and 6) to dispatch vessels to the transportation fleets.

3.2 Dynamic motion of oil films

3.2.1 Diffusion motion

Under the influence of tension, the area of the oil spill will undergo a change process from small to large in size, which is called the diffusion motion. Fay (1969) proposed a scientific oil film diffusion model, that divides the whole process into three stages according to the effects of various forces at different stages, comprehensively considering the effects of gravity, surface tension, inertial force and adhesion force. At present, the model is still used by some international mainstream oil spill prediction systems, and has quite a great deal of universal applicability. Since then, on the basis of Fay's theory, many researchers have made further explorations. After integrating the three-stage oil film diffusion model, Liu and Leendertes (1981) proposed an improved oil spill diffusion model, as follows:

$$D = f(t, Vo) = 0.61 \cdot [1.3 \cdot (\beta \cdot g \cdot Vo / \rho_0)^{1/2} \cdot t + 2.1 \cdot (\frac{\beta \cdot g \cdot Vo^2}{\rho_0^{\ 2} \cdot \sqrt{\nu_w}})^{1/3} \cdot t^{1/2} + 5.29 \cdot (\frac{\eta^2 \cdot t^3}{\rho_w^2 \cdot \nu_w})^{1/2}]^{1/2} \quad (1)$$

D is the oil film diameter; ρ_w is seawater density; ρ_0 is the oil density; β is simply a parameter, and defined by $\beta = 1 - \rho_0 / \rho_w$; g is the acceleration of gravity; Vo is the volume of oil; ν_w is the viscosity coefficient; t is the time; and η is the net surface tension coefficient. In view of its high reliability and wide application, this paper adopts the equation to present the spilled oil diffusion process.

3.2.2 Drift motion

When affected by wind, waves and currents, oil films will migrate, which is called the drift motion. The drift motion of the oil films at sea is mostly affected by geostrophic force, surface flow and sea surface wind (Chen et al., 2016). The drift velocity can be determined by the following functions:

$$\vec{u}_r = a_c \cdot \vec{u}_c + \vec{u}_w \quad (2)$$

$$\vec{u}_w = a_w \cdot \vec{u}_{10} \quad (3)$$

$\vec{u}_r$ is the velocity vector of the oil film in the sea; $\vec{u}_c$ is the surface flow velocity; a_c is the drift coefficient of surface flow; $\vec{u}_w$ is the velocity vector of wind-induced currents; a_w is the coefficient of wind-induced currents; $\vec{u}_{10}$ is the wind speed at the height of 10 m above sea level.

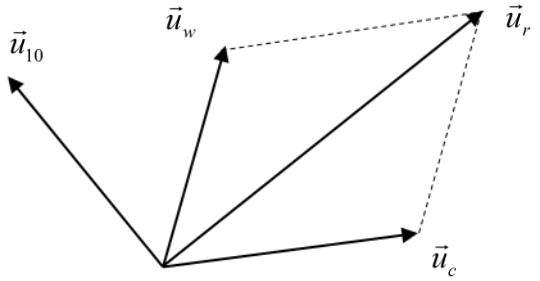

Fig. 2. Analysis diagram of drift velocity of the oil film.

3.3 Quantification of ecological loss value

In order to evaluate the value of ecological loss caused by the leakage of oil,

chemicals and other toxic materials, many researchers have proposed mature economic evaluation methods (Ando et al., 2004). Nevertheless, these methods often require a huge amount of data and take a long time to evaluate the value. Simplified formulas or models are therefore used in many American states to assess ecological damage. This kind of simplified evaluation methods has the advantages of simplicity, low cost, small demand for information and easier operation in practice. Among these models, Florida formula has been proved to be a fast and low-cost method in oil spill ecological damage assessment (Faass et al., 2010). Therefore, Florida formula is selected as the evaluation method of ecological loss in this paper. Within the context of this study, this formula is modified as follows:

$$Dam = EK \cdot M \cdot SMA \cdot PC \tag{4}$$

Dam is the value of ecological loss; *EK* is the value coefficient of different ecological environment; *M* is the area of ecological environment contaminated; *SMA* is the environmental sensitivity coefficient; *PC* is the physicochemical coefficient of the pollutant.

4 Model formulations

This paper aims to develop an efficient resource scheduling strategy for emergency logistics in response to oil spills, which respects the constraints and specifics of oil spills. Our approaches consider the complexities of the response, such as the time-varying demands of the contaminated areas, the dynamic state of the transportation networks at sea and the interrelationship between the changes in the spilled oil films and emergency operations. A dynamic optimization model for emergency resource scheduling in response to a large-scale oil spill is developed in this section. We first put forward the assumptions and define the relevant parameters and decision variables. We then propose the optimization model based on the above premises.

4.1 Assumptions

(1) The position of the demand points and the amount of the spilled oil can be identified through geographic information system (GIS), and no additional contaminated areas or spilled oil will be generated during the emergency response.

(2) External surroundings can remain stable in the emergency response, so the drift speed remains constant. Similarly, the vessels can travel at a constant speed.

(3) When a shortage of transportation capacity occurs, the ERRBs can obtain timely support from nearby ports without a waiting time. Ports have sufficient vessels to meet the replenishment needs of the ERRBs, but the operation cost of supplementary vessels is higher than that of the ERRBs' own vessels.

(4) Due to the principle of territorial management, vessels in the same fleet should be assigned by the same ERRB, and there is no situation in which a fleet is composed of vessels from multiple ERRBs. The vessels in an assembled fleet remain with the fleet until the end of the emergency response.

(5) The fleets participating in the oil spill emergency can only be constituted by the ERRBs, and the ports nearby have no right to constitute a fleet independently. While both the ports and ERRBs have the capacity to handle floating oil bladders filled with oil-water mixture.

(6) After the cleanup by skimming, the oil films will be controlled in time and the

contaminated area will not expand any more.

4.2 Notations and definitions

Sets and indices

A Set of the demand points, $a \in A = \{1, 2, \cdots, |A|\}$;

B Set of the ERRBs, $b \in B = \{|A|+1, |A|+2, \cdots, |A|+|B|\}$;

C Set of surrounding ports, $c \in C = \{|A|+|B|+1, |A|+|B|+2, \cdots, |A|+|B|+|C|\}$;

V Set of all the nodes in the transportation networks, $V = A \bigcup B \bigcup C$;

VE Set of all the nodes providing emergency services in the emergency system, $VE = B \bigcup C$;

RE Set of the emergency fleets, $re \in RE = \{1, 2, \cdots, |RE|\}$;

RT Set of the transportation fleets, $rt \in RT = \{1, 2, \cdots, |RT|\}$;

R Set of the fleets participating in the emergency response, $r \in RE \bigcup RT$;

Time-varying parameters

$dis_{ij}(t)$ Distance between nodes i and j at time t, $i, j \in V$;

$g_a(t, Vo_{at})$ Growth rate of the demand in emergency services at demand point a at time t, where Vo_{at} is the quantity of spilled oil at demand point a at time t, $a \in A$;

$tt_{(re)ij}$ Travel time required for emergency fleet re from node i to node j, $re \in RE$, $i, j \in V$;

t_{rj} Moment when fleet r arrives at node j, $r \in R$, $j \in V$;

T_{rj} Moment when fleet r is about to leave node j for the next node, $r \in R$, $j \in V$;

$tt_{(rt)ij}(m_{(re)a})$ Travel time required for transportation fleet rt from nodes i to j, when emergency fleet re services demand point a and transportation fleet rt provides it with the $m_{(re)a}$-th supplementary floating oil bladders;

$T_{(rt)j}(m_{(re)a})$ Moment when fleet rt is about to leave node j for the next node when emergency fleet re services the demand point a and transportation fleet rt provides it with the $m_{(re)a}$-th supplementary floating oil bladders.

Normal parameters

k_b Total number of vessels reserved at ERRB b, $b \in B$;

k_{re} Total number of vessels assigned to emergency fleet re, $re \in RE$;

k_{rt} Total number of vessels assigned to transportation fleet rt, $rt \in RT$;

eqk Rate of recycling oil-water mixture per vessel;

eq_{re} Rate of recycling oil-water mixture of emergency fleet re, $re \in RE$;

ek Rate of oil cleanup per vessel (i.e., the contaminated area cleaned by an emergency vessel per unit time);

e_{re} Rate of oil cleanup of emergency fleet re, $re \in RE$;

$Q_{(re)a}$ Remaining volume of floating oil bladders for emergency fleet re after completing emergency operations at point a, $re \in RE$, $a \in A$;

$Q_{(re)(\xi\text{-}a)}$ Remaining volume of floating oil bladders for emergency fleet re after completing emergency operations at the point just before point a, $re \in RE$, $\xi\text{-}a \in A$;

$t(m_{(re)a})$ Moment when emergency fleet re services demand point a at the $m_{(re)a}$-th time a shortage occurs in the capacity of floating oil bladders;

$m_{(re)a}$ Ordinal number of the capacity shortages in floating oil bladders when emergency fleet *re* services demand point *a,* with $m_{(re)a}=\{0,1,2\cdots,n_{(re)a}\}$, where $n_{(re)a}$ is the maximum ordinal number in this case and if $n_{(re)a}=0$, a shortage never occurs, $re \in RE$, $a \in A$;

v_j Drift velocity of the oil film at point j ($j \in A$);

vk Speed of the vessels;

NK Positive integer representing the maximum number of vessels allowed per fleet;

qe Maximum capacity of floating oil bladders carried by an emergency vessel;

qt Maximum capacity of floating oil bladders carried by a transportation vessel;

ock Fixed operating cost of the emergency vessels owned by the ERRBs;

sck Fixed operating cost of the emergency vessels temporarily acquired from the nearby ports;

ct Travel cost per nautical mile of a vessel;

$\hat{T}$ Time difference between the completion of contaminated area monitoring and the beginning of emergency operations;

EK Value coefficient of the different ecological environments;

SMA Environmental sensitivity coefficient;

PC Physicochemical coefficient of the pollutant.

Decision Variables

u_{rb} 1, if fleet *r* is contributed by ERRB *b*, and 0 otherwise, $r \in R$, $b \in B$;

$y_{(re)ij}$ 1, if emergency fleet *re* travels from nodes *i* to *j*, and 0 otherwise, $re \in RE$, $i, j \in V$;

$z_{(re)a}$ 1, if emergency fleet *re* is responsible for demand point *a*, and 0 otherwise, $re \in RE$, $a \in A$;

$l_{(rt)ij}(m_{(re)a})$ 1, if transportation fleet *rt* travels from nodes *i* to *j* on the way to transport floating oil bladders when emergency fleet *re* services demand point *a* at the $m_{(re)a}$-th time a shortage occurs in the capacity of floating oil bladders, and 0 otherwise, $re \in RE$, $rt \in RT$, $i, j \in V$;

$h_{(rt)a}(m_{(re)a})$ 1, if transportation fleet *rt* provides supplies to demand point *a* when emergency fleet *re* services demand point *a* at the $m_{(re)a}$-th time a shortage occurs in the capacity of floating oil bladders, and 0 otherwise, $re \in RE$, $rt \in RT$, $i \in B$, $a \in A$;

k_{re} Number of vessels assigned to emergency fleet *re*, $re \in RE$;

k_{rt} Number of vessels assigned to transportation fleet *rt*, $rt \in RT$.

4.3 Optimization model of emergency resource scheduling

4.3.1 Objective functions

Through reviewing the recent studies on land-based emergency logistics (Ahmadi et al., 2015; Moreno et al., 2018; Maharjan et al., 2020; Zhang et al., 2019) and maritime emergency logistics (Xu et al., 2016; Li et al., 2014a), it can be demonstrated that a successful sudden-onset disaster response should meet the needs of effectiveness in the shortest amount of time (responsiveness) with the least amount of resources (cost efficiency) (Hu et al., 2016; Kunz et al., 2017; Baharmand, 2019). Therefore, responsiveness and the response cost are both considered as the optimization objectives in this paper. The two objectives have conflicting nature, which decision makers need

to strike a balance to pursue the optimal scheme for oil spill emergency.

Objective 1: Minimization of the value of the ecological loss caused by oil spill pollution

The first objective is mostly reflected in the value of ecological loss caused by oil spill pollution. The higher the efficiency, the more quickly spilled oil can be controlled and cleaned, and thus the smaller the ecological loss will be. This value is directly determined by the area contaminated by the oil films. When emergency fleet *re* has completed its cleanup operations at demand point *a*, the area eventually contaminated at demand point *a* is simply the area cleaned by emergency fleet *re*. Therefore, based on Equation (4), the first objective function is formulated as follows:

$$\min\ Z_1 = \sum_{a\in A}\sum_{re\in RE} EK\cdot SMA\cdot PC\cdot (T_{(re)a} - t_{(re)a})\cdot e_{re}\cdot z_{(re)a} \tag{5}$$

Objective 2：Minimization of the total response cost

The total response cost generated during the emergency response mostly includes the fixed operation cost of the vessels and the vessel travel cost. Specifically, the total cost consists of five components, namely, the fixed operating cost of the vessels owned by the ERRBs, the fixed operating costs of any temporarily requisitioned vessels from nearby ports, the generated travel cost of the emergency fleets between the network nodes, the generated travel cost of the emergency fleets with the oil film drift, and the generated travel cost of transportation fleets between the network nodes. The second objective function is thus presented as follows:

$$\begin{aligned}\min\ Z_2 &= \sum_{b\in B} ock\cdot \min\left\{\sum_{r\in R} k_r\cdot x_{rb}\ ,\ k_b\right\} + \sum_{b\in B} sck\cdot \max\left\{(\sum_{r\in R} k_r\cdot x_{rb} - k_b)\ ,\ 0\right\}\\ &+ \sum_{re\in RE}\sum_{i\in V}\sum_{j\in V} ct\cdot vk\cdot tt_{(re)ij}\cdot y_{(re)ij} + \sum_{re\in RE}\sum_{i\in A} ct\cdot v_i\cdot\left(T_{(re)i} - t_{(re)i}\right)\cdot z_{(re)i}\\ &+ \sum_{re\in RE}\sum_{rt\in RT}\sum_{i\in V}\sum_{j\in V}\sum_{a\in A}\sum_{m_{(re)a}=1}^{n_{(re)a}} ct\cdot vk\cdot tt_{(rt)ij}(m_{(re)a})\cdot l_{(rt)ij}(m_{(re)a})\cdot z_{(re)a}\cdot h_{(rt)a}(m_{(re)a})\end{aligned} \tag{6}$$

To minimize the first objective function, the time required to recycle the spilled oil has to be decreased as much as possible. This cannot be achieved unless the largest amount of emergency resources is invested in the emergency response to complete the cleanup as soon as possible. Nevertheless, this contradicts the nature of the second objective function, which aims to minimize the total response cost.

4.3.2 Constraints of the multi-objective model

$$t_{(re)j} = \sum_{i\in V}(T_{(re)i} + tt_{(re)ij})\cdot y_{(re)ij}\ ,\quad \forall re\in RE\quad \forall i,j\in V \tag{7}$$

$$t_{rij} = F(T_{ri})\qquad \forall r\in R\ ,\quad \forall i,j\in V \tag{8}$$

Constraint (7) defines the moment when emergency fleet *r* reaches node *j*. Constraint (8) defines the travel time of the fleets between the nodes, and the specific expansion is explained below referring to Equation (35).

$$T_{(re)i} = 0\ ,\forall re\in RE\ ,\forall i\in B \tag{9}$$

$$z_{(re)i}\cdot\int_0^{t_{(re)i}+\hat{T}} g_i(t,Vo_{at})\mathrm{d}t = z_{(re)i}\cdot\int_{t_{(re)i}+\hat{T}}^{T_{(re)i}+\hat{T}}\left(e_{re} - g_i(t,\bar{Vo}_{at})\right)\mathrm{d}t\ ,\forall re\in RE\quad ,\quad \forall i\in A \tag{10}$$

Constraints (9) and (10) define the moment when the emergency fleets leave each node for the next node, where $g_i(t,Vo_{at})$ is determined by *t* and Vo_{at}. Since Vo_{at} varies

over time under skimming, it is replaced by the mean quantity of the initial and final spilled oil quantity at demand point a. Because the oil film at demand point a will be completely cleaned under ideal conditions, the final spilled oil quality is zero, which results in the mean quantity being half of the initial spilled oil quantity.

$$z_{(re)i} \cdot e_{re} \geq z_{(re)i} \cdot g_i(t, Vo_{it}), \quad \forall re \in RE \quad , \quad \forall i \in A \tag{11}$$

$$e_{re} = k_{re} \cdot ek, \quad \forall re \in RE \tag{12}$$

Constraint (11) stipulates that the efficiency of the emergency fleet must be higher than the growth rate of the demand for emergency services at the demand point it is responsible for in terms of cleanup. Constraint (12) defines the rate of oil cleanup for emergency fleet *re*.

$$k_{re} \leq NK, \quad \forall re \in RE \tag{13}$$

Constraint (13) stipulates that the maximum number of vessels allowed per emergency fleet must not exceed *NK* due to the budget constraints and limited resources.

$$\frac{\pi}{4} \cdot \left(f(t, Vo_{at}) \right)^2 = \int_0^t g_a(t, Vo_{at}) \mathrm{d}t, \quad \forall a \in A \tag{14}$$

Constraint (14) defines the growth rate of demand for emergency services at demand point *a* at time *t* and $f(t, Vo_{at})$, which is expressed in Equation (1).

$$\sum_{j \in A} y_{(re)ij} = u_{(re)i}, \forall re \in RE \quad , \quad \forall i \in B \tag{15}$$

$$\sum_{r \in R} y_{rij} = 0, \quad \forall i, j \in B \tag{16}$$

$$\sum_{i \in V} y_{rij} - \sum_{i \in V} y_{rji} = 0, \quad \forall r \in R, \quad \forall j \in V \tag{17}$$

$$\sum_{i \in V} y_{(re)ij} + \sum_{i \in V} y_{(re)ji} \leq 2, \quad \forall re \in RE, \forall j \in V \tag{18}$$

Constraint (15) stipulates that the origin of an emergency fleet contributed by ERRB *i* is just ERRB *i*. Constraint (16) indicates that the fleet does not travel between the ERRBs. Constraint (17) represents fleet flow conservation. Constraint (18) indicates that each node allows the emergency fleet to pass no more than once, to eliminate any route subloops and avoid the establishment of a circular route, which does not pass along the ERRBs.

$$\sum_{re \in RE} z_{(re)a} = 1, \quad \forall re \in RE, \quad \forall a \in A \tag{19}$$

Constraint (19) indicates that each demand point is served by one and only one emergency fleet.

$$y_{(re)ij} \cdot \left(t_{(re)j} - t_{(re)i} \right) \geq 0, \quad \forall re \in RE, \quad \forall i, j \in V \tag{20}$$

Constraint (20) indicates that the nodes along the route of the emergency fleets occur sequentially.

$$\sum_{rt \in RT} \sum_{m_{(re)a}=1}^{n_{(re)a}} h_{(rt)a}(m_{(re)a}) \cdot z_{(re)a} = n_{(re)a} \cdot z_{(re)a} \quad , \quad \forall re \in RE, \quad \forall a \in A \tag{21}$$

$$\sum_{rt \in RT} h_{(rt)a}(m_{(re)a}) \cdot z_{(re)a} = 1, \quad \forall re \in RE, \quad m_{(er)a} \geq 1 \tag{22}$$

Constraints (21) and (22) indicate that when emergency fleet *re* faces a short-term capacity in floating oil bladders for the $m_{(re)a}$-th time, one and only one transportation fleet is assigned to provide supplementary floating oil bladders.

$$\sum_{rt \in RT} \sum_{i \in B} \left[T_{(rt)i}(m_{(re)a}) + tt_{(rt)ia}(m_{(re)a}) \right] \cdot h_{(rt)a}(m_{(re)a}) \cdot l_{(rt)ia}(m_{(re)a}) \cdot z_{(re)a} \leq t(m_{(re)a}) \cdot z_{(re)a}$$

$$\forall re \in RE,\ a \in A,\ T_{(rt)i}(m_{(re)a}) = 0,\ m_{(re)a} \geq 1 \tag{23}$$

$$\sum_{rt \in RT} \sum_{j \in VE} \left[T_{(rt)i}(m_{(re)a}) + tt_{(rt)ij}(m_{(re)a}) + tt_{(rt)ja}(m_{(re)a}) \right] \cdot h_{(rt)a}(m_{(re)a}) \cdot l_{(rt)ij}(m_{(re)a}) \cdot l_{(rt)ja}(m_{(re)a}) \cdot z_{(re)a} \leq t(m_{(re)a}) \cdot z_{(re)a}$$

$$\forall re \in RE,\ i \in V,\ a \in A,\ T_{(rt)i}(m_{(re)a}) > 0,\ m_{(re)a} \geq 1 \tag{24}$$

Constraints (23) and (24) define the time window for the transportation fleet to transport supplies to the emergency fleet to avoid emergency operation stagnation. Constraint (23) defines the time window when the transportation fleet first leaves its origin ERRB when transporting supplies to the emergency fleet, while Constraint (24) defines the time window in the other cases.

$$\left\lceil \frac{\max\left\{ (T_{(re)a} - t_{(re)a}) \cdot eqk \cdot k_{re} - Q_{(re)(\xi - i)},\ 0 \right\}}{qe \cdot k_{re}} \right\rceil \cdot z_{(re)a} = n_{(re)a},\quad \forall re \in RE,\quad a \in A \tag{25}$$

$$\sum_{m_{(re)a}=1}^{n_{(re)a}} qe \cdot k_{re} \cdot z_{(re)a} + Q_{(re)(\xi\text{-}a)} - \left(T_{(re)a} - t_{(re)a} \right) \cdot eqk \cdot k_{re} \cdot z_{(re)a} = Q_{(re)a}$$

$$\forall re \in RE,\quad a \in A,\quad \xi\text{-}a \in A,\quad n_{(re)a} \geq 1 \tag{26}$$

$$\sum_{rt \in RT} k_{rt} \cdot qt \cdot h_{(rt)a}(m_{(re)a}) \cdot z_{(re)a} \geq k_{re} \cdot qe \cdot z_{(re)a} \quad \forall re \in RE,\ \forall a \in A,\ m_{(er)a} \geq 1 \tag{27}$$

Constraint (25) defines the maximum ordinal number of the shortages in capacity of floating oil bladders when emergency fleet *re* services demand point *a*. Constraint (26) denotes the remaining volume of floating oil bladders for emergency fleet *re* after completing its emergency operations at point *a*. Constraint (27) requires the capacity of floating oil bladders carried by transportation fleet *rt* to be no lower than that of emergency fleet *re*.

$$u_{ri} \in \{0,\ 1\},\ \forall r \in R,\ \forall i \in B \tag{28}$$

$$y_{(re)ij} \in \{0,\ 1\},\ \forall re \in RE\ ,\forall i, j \in V \tag{29}$$

$$z_{(re)i} \in \{0,\ 1\}\ ,\ \forall re \in RE,\ \forall i \in A \tag{30}$$

$$l_{(rt)ij}(m_{(re)a}) \in \{0,\ 1\},\ \forall re \in RE,\ \forall i, j \in V,\ \forall a \in A,\ m_{(er)a} \geq 1 \tag{31}$$

$$h_{(rt)a}(m_{(er)a}) \in \{0,\ 1\},\ \forall re \in RE,\ \forall a \in A\ ,\ m_{(er)a} \geq 1 \tag{32}$$

Binary integer constraints for the various decision variables are given in Constraints (28)-(32).

In addition, oil films always drift due to the influence of external surroundings at sea. When fleet *r* completes its emergency operations at the current demand point *i* and travels to the next demand point *j*, the travel distance continuously changes. To determine the travel time of the emergency fleets between the different nodes, we provide a detailed explanation in the form of a mathematical derivation, and the position of the nodes at sea is shown in Fig. 3, where a_i is the position of point *i*, a_j is that of point *j* and a_j^* is the location where the fleet meets point *j*.

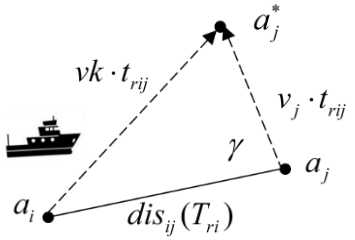

Fig. 3. Stroke diagram of the dynamic route.

Based on the cosine theorem, the following equation is proposed:

$$\begin{aligned}&\left(vk\cdot tt_{rij}\right)^2=dis_{ij}^2(T_{ri})+\left(v_j\cdot tt_{rij}\right)^2-2\cdot dis_{ij}(T_{ri})\cdot v_j\cdot tt_{rij}\cdot\cos\gamma\\&\Rightarrow tt_{rij}=\frac{-v_j\cdot dis_{ij}(T_{ri})\cdot\cos\gamma\pm dis_{ij}(T_{ri})\cdot\sqrt{vk^2-v_j^2\cdot\sin^2\gamma}}{vk^2-v_j^2}\end{aligned}\tag{33}$$

According to Equation (33), the following speed constraint must be satisfied when fleet r is able to travel to point j:

$$vk^2-v_j^2\cdot\sin^2\gamma\geq 0\Rightarrow vk\geq v_j\cdot\sin\gamma\tag{34}$$

Therefore, the function of the travel time between the nodes is formulated as follows:

$$tt_{rij}=F(T_{ri})=\frac{-v_j\cdot dis_{ij}(T_{ri})\cdot\cos\gamma+dis_{ij}(T_{ri})\cdot\sqrt{vk^2-v_j^2\cdot\sin^2\gamma}}{vk^2-v_j^2},\quad\forall r\in R,\quad\forall i,j\in V\tag{35}$$

5 Solution procedure

To solve the proposed model which contains a number of parameters with time coupling, we convert it into a two-stage counterpart, which yields the same optimal solutions and retains the calculation logic of the problem identical.

5.1 Hybrid heuristic algorithm

The first-stage model determines the origin ERRB of each emergency fleet, plans the routes and dispatches the vessels to the emergency fleets. When an emergency fleet exhibits an insufficient capacity of floating oil bladders in the scheduling scheme developed by the first-stage model, the second-stage model is triggered to formulate decisions related to the transportation fleets to provide supplementary empty floating oil bladders and handle fully loaded ones.

The first-stage model is developed as:

$$\min\ \mathrm{Z}_1=\sum_{a\in A}\sum_{re\in RE}EK\cdot SMA\cdot PC\cdot(T_{(re)a}-t_{(re)a})\cdot e_{re}\cdot z_{(re)a}\tag{36}$$

$$\min\ \mathrm{Z}_2=\sum_{re\in RE}\sum_{i\in V}\sum_{j\in V}ct\cdot vk\cdot tt_{(re)ij}\cdot y_{(re)ij}+\sum_{re\in RE}\sum_{i\in A}ct\cdot v_i\cdot\left(T_{(re)i}-tt_{(re)i}\right)\cdot z_{(re)i}+\mathrm{Z}_3\tag{37}$$

$$t_{(re)j}=\sum_{i\in V}(T_{(re)i}+t_{(re)ij})\cdot y_{(re)ij},\quad\forall i,j\in V\tag{38}$$

$$tt_{(re)ij}=F(T_{ri})=\frac{-v_j\cdot dis_{ij}(T_{(re)i})\cdot\cos\gamma+dis_{ij}(T_{(re)i})\cdot\sqrt{vk^2-v_j^2\cdot\sin^2\gamma}}{vk^2-v_j^2},$$

$$\forall re\in RE,\quad\forall i,j\in V\tag{39}$$

$$T_{(re)i}=0,\quad\forall re\in RE,\quad\forall i\in B\tag{40}$$

$$z_{(re)i}\cdot\int_0^{t_{(re)i}+\hat{T}}g_i(t,Vo_{at})\mathrm{d}t=z_{(re)i}\cdot\int_{t_{(re)i}+\hat{T}}^{T_{(re)i}+\hat{T}}\left(e_{re}-g_i(t,\bar{V}o_{at})\right)\mathrm{d}t,\quad\forall re\in RE,\quad\forall i\in A\tag{41}$$

$$z_{(re)i}\cdot e_{re}\geq z_{(re)i}\cdot g_i(t,Vo_{it}),\quad\forall re\in RE\quad,\quad\forall i\in A\tag{42}$$

$$e_{re}=k_{re}\cdot ek,\quad\forall re\in RE\tag{43}$$

$$k_{re} \le NK, \quad \forall re \in RE \tag{44}$$

$$\frac{\pi}{4} \cdot \left(f(t, Vo_{at}) \right)^2 = \int_0^t g_a(t, Vo_{at}) \mathrm{d}t, \quad \forall a \in A \tag{45}$$

$$\sum_{j \in A} y_{(re)ij} = u_{(re)i}, \forall re \in RE \quad , \forall i \in B \tag{46}$$

$$\sum_{r \in R} y_{rij} = 0, \quad \forall i, j \in B \tag{47}$$

$$\sum_{i \in V} y_{rij} - \sum_{i \in V} y_{rji} = 0, \quad \forall r \in R, \quad \forall j \in V \tag{48}$$

$$\sum_{i \in V} y_{(re)ij} + \sum_{i \in V} y_{(re)ji} \le 2, \quad \forall re \in RE, \quad \forall j \in V \tag{49}$$

$$\sum_{re \in RE} z_{(re)a} = 1, \quad \forall a \in A \tag{50}$$

$$y_{(re)ij} \cdot \left(t_{(re)j} - t_{(re)i} \right) \ge 0, \quad \forall re \in RE, \quad \forall i, j \in V \tag{51}$$

$$u_{(re)i} \in \{0, 1\}, \quad \forall re \in RE, \forall i \in B \tag{52}$$

$$y_{(re)ij} \in \{0, 1\}, \quad \forall re \in RE \quad , \forall i, j \in V \tag{53}$$

$$z_{(re)i} \in \{0, 1\} \quad , \quad \forall re \in RE, \forall i \in A \tag{54}$$

Objective function (36) expresses the minimum value of the ecological loss caused by the oil spills during the emergency response. Objective function (37) represents the minimum total response cost, and the meaning of each part is consistent with that in objective function (6). However, Z_3 cannot be determined until the completion of the second-stage model, which expresses the operation cost of all fleets and the logistics cost related to the transportation fleets. Constraints (38)-(54) have been defined in Section 4.3. In essence, it is a multi-objective location-routing model. Since multi-objective particle swarm optimization (MPSO) attains a high convergence rate, good robustness and notable global search ability, and avoids any complex genetic operations similar to the genetic algorithm, MPSO is adopted to solve the first-stage model. However, conventional multi-objective particle swarm optimization (CMPSO) easily falls into the local optima in the late search process. To improve the search ability of the algorithm and ensure the diversity of Pareto non-dominated solutions, we propose an improved particle swarm optimization (IMPSO) for solving the model.

The second-stage model is developed as follows:

$$\begin{aligned} \min \ Z_3 = & \sum_{b \in B} ock \cdot \min \left\{ \sum_{r \in R} k_r \cdot x_{rb}, \ k_b \right\} + \sum_{b \in B} sck \cdot \max \left\{ \left(\sum_{r \in R} k_r \cdot x_{rb} - k_b \right), \ 0 \right\} + \\ & \sum_{re \in RE} \sum_{rt \in RT} \sum_{i \in V} \sum_{j \in V} \sum_{a \in A} \sum_{m_{(re)a}=1}^{n_{(re)a}} ct \cdot vk \cdot tt_{(rt)ij}(m_{(re)a}) \cdot l_{(rt)ij}(m_{(re)a}) \cdot z_{(re)a} \cdot h_{(rt)a}(m_{(re)a}) \end{aligned} \tag{55}$$

$$\sum_{rt \in RT} \sum_{m_{(re)a}=1}^{n_{(re)a}} h_{(rt)a}(m_{(re)a}) \cdot z_{(re)a} = n_{(re)a} \cdot z_{(re)a} \quad , \quad \forall re \in RE, \quad \forall a \in A \tag{56}$$

$$\sum_{rt \in RT} h_{(rt)a}(m_{(re)a}) \cdot z_{(re)a} = 1, \quad \forall re \in RE, \quad m_{(re)a} \ge 1 \tag{57}$$

$$tt_{(rt)ij}(t(m_{(re)a})) = \frac{-v_j \cdot dis_{ij}(t(m_{(re)a})) \cdot \cos\gamma + dis_{ij}(t(m_{(re)a})) \cdot \sqrt{vk^2 - v_j^2 \cdot \sin^2\gamma}}{vk^2 - v_j^2} \cdot z_{(re)a}$$
$$\forall rt \in RT, \quad \forall re \in RE, \quad \forall a \in A, \quad \forall i, j \in V \tag{58}$$

$$\sum_{rt\in RT}\sum_{i\in B}\left[T_{(rt)i}(m_{(er)a})+tt_{(rt)ia}(m_{(er)a})\right]\cdot h_{(rt)a}(m_{(er)a})\cdot l_{(rt)ia}(m_{(re)a})\cdot z_{(re)a}\le t(m_{(er)a})\cdot z_{(re)a}$$

$$\forall re\in RE,\ \ a\in A,\ \ T_{(rt)i}(m_{(re)a})=0,\ \ m_{(er)a}\ge 1 \tag{59}$$

$$\sum_{rt\in RT}\sum_{j\in VE}\left[T_{(rt)i}(m_{(er)a})+tt_{(rt)ij}(m_{(er)a})+tt_{(rt)ja}(m_{(er)a})\right]\cdot h_{(rt)a}(m_{(er)a})\cdot l_{(rt)ij}(m_{(re)a})\cdot l_{(rt)ja}(m_{(re)a})\cdot z_{(re)a}\le t(m_{(er)a})\cdot z_{(re)a}$$

$$\forall re\in RE,\ \ i\in V,\ \ a\in A,\ \ T_{(rt)i}(m_{(re)a})>0,\ \ m_{(er)a}\ge 1 \tag{60}$$

$$\left\lceil\frac{\max\left\{(T_{(re)a}-t_{(re)a})\cdot eqk\cdot k_{re}-Q_{(re)(\xi-i)}\ ,\ 0\right\}}{qe\cdot k_{re}}\right\rceil\cdot z_{(re)a}=n_{(re)a},\quad \forall re\in RE,\quad a\in A \tag{61}$$

$$\sum_{m_{(re)a}=1}^{n_{(re)a}} qe\cdot k_{re}\cdot h_{(rt)a}(m_{(re)a})\cdot z_{(re)a}+Q_{(re)(\xi\text{-}a)}-\left(T_{(re)a}-t_{(re)a}\right)\cdot eqk\cdot k_{re}\cdot z_{(re)a}=Q_{(re)a}$$

$$\forall re\in RE,\quad a\in A,\quad \xi\text{-}a\in A,\quad n_{(re)a}\ge 1 \tag{62}$$

$$\sum_{rt\in RT}k_{rt}\cdot qt\cdot h_{(rt)a}(m_{(re)a})\cdot z_{(re)a}\ge k_{re}\cdot qe\cdot z_{(re)a},\ \ \forall re\in RE,\ \ \forall a\in A,\ \ m_{(er)a}\ge 1 \tag{63}$$

$$l_{(rt)ij}(m_{(re)a})\in\{0\ ,\ 1\},\ \ \forall re\in RE,\ \ \forall i,j\in V,\ \ \forall a\in A,\ \ m_{(er)a}\ge 1 \tag{64}$$

$$h_{(rt)a}(m_{(er)a})\in\{0\ ,\ 1\},\ \ \forall re\in RE,\ \ \forall a\in A\ \ ,\ \ m_{(er)a}\ge 1 \tag{65}$$

Objective function (55) mostly compromises the operation cost of all fleets and the logistics cost of the transportation fleets, and combined objective function (37), it constitutes the objective function of the total response cost. Constraints (56) - (65) have been defined in Section 4.3. The optimization objective of the second-stage model is mostly determined by the total cost of the transportation fleets. Therefore, the optimization objective of the second-stage model is achieved based on the transportation fleets with the minimal total operating cost and by planning the shortest transportation routes on the premise that the responsiveness of the emergency fleets is not affected. During the response phase, each transportation fleet provides supplementary floating oil bladders to the emergency fleets on several occasions from different nodes in the emergency logistics networks. Therefore, the optimization problem is essentially a multi-source shortest-path problem. Since the Floyd algorithm has been applied as a basic tool for multi-source shortest-path problem (Zhao et al., 2019), it is adopted to solve the second-stage model in this paper as well.

To resolve the two-stage model, a hybrid heuristic algorithm (HHA) is proposed, which combines the above two independent algorithms to achieve the purpose of overall optimization in an organic way. The HHA is also composed of two stages, similar to the transformed model, whose upper layer involves the IMPSO algorithm, while the lower layer contains the Floyd algorithm. A calculation flow chart of the HHA is shown in Fig. 4, and the detailed procedure is described in the following sections.

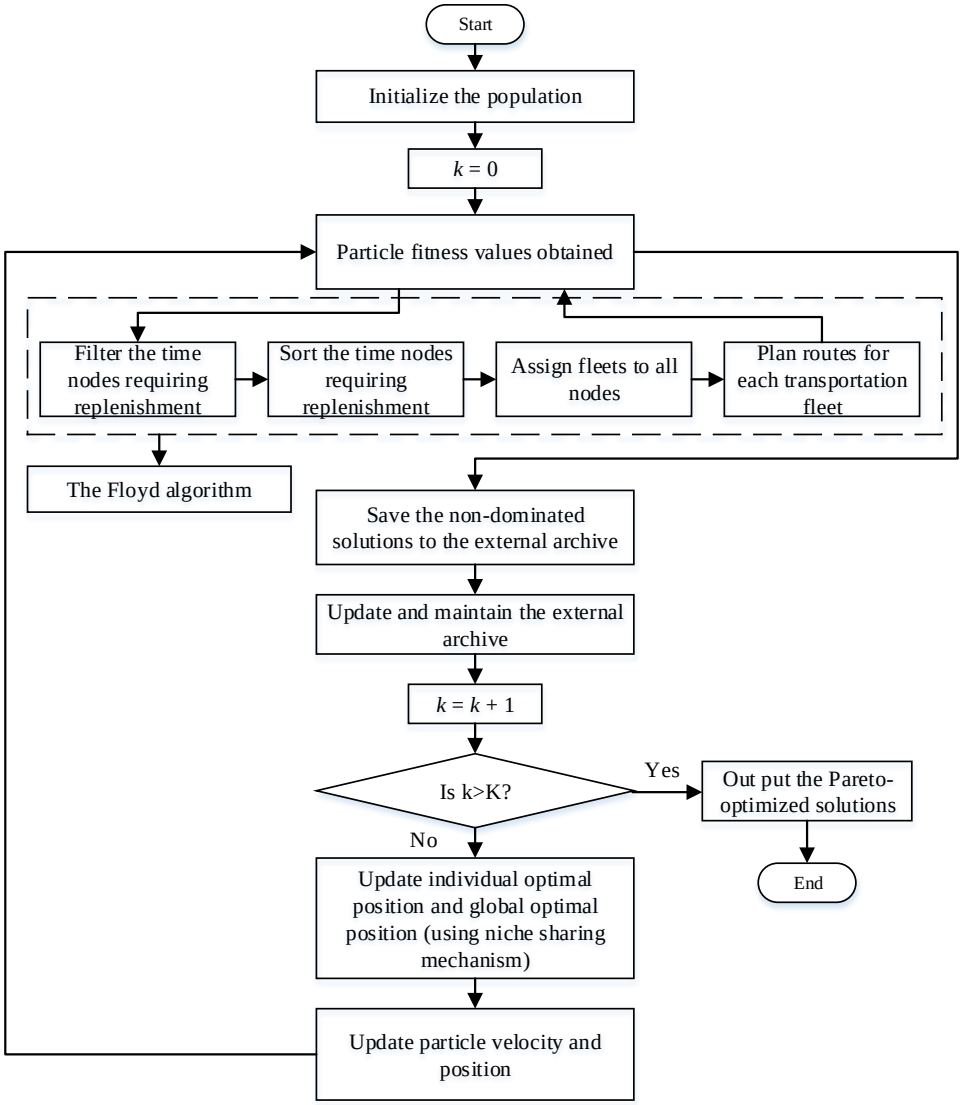

Fig. 4. Flow chart of the HHA combining IMPSO with the Floyd algorithm

5.2 The IMPSO algorithm

5.2.1 Standard PSO

The standard PSO algorithm is an intelligent optimization algorithm that simulates the behavior of birds in flight and searches for the optimal solution through the cooperation among particles (Kennedy and Eberhart, 1995). In this algorithm, solutions to the optimization problem are regarded as particles in the search space, and the optimal solution is obtained by continuous iteration. During the iteration process, each particle updates its own position and generates a new particle for the next generation by tracking individual optimal position p_{i} and global optimal position p_{g}. Let the number of particles in population be N, where the velocity and position of the i-th particle after the τ- th iteration in D-dimensional space are $v_i^{\tau} = \left[v_{i1}^{\tau}, v_{i2}^{\tau}, \cdots, v_{id}^{\tau}, \cdots, v_{iD}^{\tau} \right]$ and $x_i^{\tau} = \left[x_{i1}^{\tau}, x_{i2}^{\tau}, \cdots, x_{id}^{\tau}, \cdots, x_{iD}^{\tau} \right]$ respectively. In standard PSO, the updated functions for the velocity and position of particles are formulated as follows:

$$v_{id}^{\tau+1} = \omega \cdot v_{id}^{\tau} + c_1 \cdot r_1 \cdot (p_{id}^{\tau} - x_{id}^{\tau}) + c_2 \cdot r_2 \cdot (p_{gd}^{\tau} - x_{id}^{\tau})$$

$$v_{id}^{\tau+1} = \begin{cases} v_{\max} , \ if \ v_{id}^{\tau+1} > v_{\max} \\ -v_{\max} , \ if \ v_{id}^{\tau+1} < -v_{\max} \end{cases} \tag{66}$$

$$x_{id}^{\tau+1} = x_{id}^{\tau} + v_{id}^{\tau+1} \tag{67}$$

ω is the inertial weight and $\omega = \omega_{\max} - (\omega_{\max} - \omega_{\min}) \cdot \frac{\tau}{\mathrm{T}}$ where $\omega_{\max}$ and $\omega_{\min}$ are the maximum and minimum weights respectively. τ is the current number of iterations and T is the maximum number of iterations. c_1 and c_2 are the learning factors, which are usually set as $0 < c_1, c_2 < 2$ to ensure algorithm convergence. r_1 and r_2 are random numbers evenly distributed between 0 and 1. $v_{\max}$ is the limitation of maximum speed, which determines the search accuracy of particles in the feasible region. The optimal solution obtained by particle *i* after the τ-th iteration is the individual optimal solution $Pbest_i$, and its position is $p_i^{\tau} = [p_{i1}^{\tau}, p_{i2}^{\tau}, \cdots, p_{id}^{\tau}, \cdots, p_{iD}^{\tau}]$. While the optimal solution found for the whole population is the global optimal solution $Gbest$, and its position is $p_g^{\tau} = [p_{g1}^{\tau}, p_{g2}^{\tau}, \cdots, p_{gd}^{\tau} \cdots, p_{gD}^{\tau}]$.

When dealing with multi-objective optimization problems, the global optimal position is no longer unique, and there are multiple solutions among which no one is superior to the others. The selection and preservation of p_i and p_g is the key issue in transforming standard PSO into MPSO. In CMPSO, these values are randomly selected (Zhang et al., 2017). During the iteration, when too many particles are gathered in a local area of the external archive, the probability of the global optimal position coming from this area will increase greatly. Thus, the particles in the whole iteration process are guided to move toward this region so that the local convergence and prematurity of the calculation easily occur. To avoid such issues, we propose IMPSO with better search ability, which adopts the niche sharing mechanism to select the global optimal position.

5.2.2 Introduction of the niche sharing mechanism

According to the niche sharing mechanism, the fitness of particle x_i^{τ} in the external archive is defined as follows:

$$F_i = \frac{1}{S_i}, \ i = 1, 2, \cdots, N_s \tag{68}$$

N_s is the total number of particles in the current external archive, and S_i is the sharing degree of particle x_i^{τ}, which can be formulated as follows:

$$S_i = \sum_{j=1}^{N_s} f_{sh}(d_{ij}), \ i = 1, 2, \cdots, N_s \tag{69}$$

$f_{sh}(d_{ij})$ is the shared function between particles x_i^{τ} and x_j^{τ}, and represents the degree of closeness between them. The function is defined as follows:

$$f_{sh}(d_{ij}) = \begin{cases} 1 - (\frac{d_{ij}}{\sigma_{share}})^{\beta}, \ 0 \le d_{ij} < \sigma_{share} \\ 0 \quad , \ d_{ij} \ge \sigma_{share} \end{cases} \tag{70}$$

β is the parameter that controls the shape of the shared function, usually set as 1 or 2.

σ_{share} is the shared distance. d_{ij} is the distance between particles x_i^τ and x_j^τ, which is usually measured by the Euclidean distance:

$$d_{ij} = \left\| x_i^\tau - x_j^\tau \right\| = \sqrt{\sum_{d=1}^{D} (x_{id}^\tau - x_{jd}^\tau)^2} \tag{71}$$

When some particles in the external archive appear to aggregate, the degree of sharing among particles there will increase significantly, and their fitness value in the niche will decrease accordingly, and vice versa. In the iteration of MPSO, this method can be used to evaluate the fitness of the particles in the external archive, and then to select the proper particle as the global optimal position p_g^τ following the principle of roulette selection. This method can effectively reduce the probability of similar particles being selected in the iteration, to ensure the diversity of particles in the evolutionary process and to avoid the occurrence of local convergence and prematurity.

5.2.3 Particle coding operations

In this paper, we adopt decimal particle coding to represent the solutions in IMPSO. Each encoding sequence denotes an emergency fleet scheduling scheme for a large-scale oil spill accident. Each particle is represented by x_i^τ defined in Section 5.2.1. Specifically, the encoding sequence of each particle consists of four sub-strings as shown in Equation (72), and the total number of the code bits is D.

$$x_i^\tau = \{\underbrace{(x_{i11}^\tau, x_{i12}^\tau, \cdots, x_{i1n}^\tau)}_{x_{i1}^\tau}, \underbrace{(x_{i21}^\tau, x_{i22}^\tau, \cdots, x_{i2n}^\tau)}_{x_{i2}^\tau}, \underbrace{(x_{i31}^\tau, x_{i32}^\tau, \cdots, x_{i3l}^\tau)}_{x_{i3}^\tau}, \underbrace{(x_{i41}^\tau, x_{i42}^\tau, \cdots, x_{i4l}^\tau)}_{x_{i4}^\tau}\} \tag{72}$$

The encoding sequence of the particle is a D-dimensional vector with each bit randomly generated between 0 and 1. The numbers of code bits in sub-strings x_{i1}^τ and x_{i2}^τ are both *n*, the same as that of demand points. Both sub-string x_{i3}^τ and x_{i4}^τ are sequences with *l* bits, the same number as that of the emergency fleets. Thus, each encoding sequence of the particle (given by $n + n + l + l$=D) is a D-dimensional vector.

Sub-strings x_{i1}^τ and x_{i2}^τ together make the routing decisions for each emergency fleet. Sub-string x_{i1}^τ will be multiplied by *l* and rounded up. The codes of sub-string x_{i2}^τ will be converted into random numbers from 1 to *n* according to the rank of the decimals of each coding bit in the sequence in order from small to large. The emergency fleet denoted by the first bit in sub-string x_{i1}^τ is responsible for the demand point denoted by the first bit in sub-string x_{i2}^τ; the emergency fleet denoted by the second bit in sub-string x_{i1}^τ is responsible for the demand point denoted by the second bit in sub-string x_{i2}^τ, and so forth.

Sub-string x_{i3}^τ makes the location decisions for each fleet's origin ERRB, by which each fleet is constituted. The codes of sub-string x_{i3}^τ will be converted into random numbers from 1 to *m* (the total number of the candidate ERRBs) by multiplying the codes with *m* and rounding up. The ERRB denoted by the first bit in sub-string x_{i3}^τ is responsible for constituting the first emergency fleet; the ERRB denoted by the second bit in sub-string x_{i3}^τ is responsible for constituting the second emergency fleet, and so forth.

Sub-string x_{i4}^τ is used to determine the number of vessels to be assigned to each emergency fleet. The codes of sub-string x_{i4}^τ will be converted into random numbers

within the acceptable interval, which indicates the number of vessels assigned to an emergency fleet is constrained in accordance with Constraint (42)-(44).

5.2.4 The procedure of the IMPSO algorithm

The steps of the IMPSO are described as follows:

Step 1: The population is initialized. The initial position x_i^0 and initial velocity v_i^0 of N particles are randomly generated. The optimal position of an initialized particle is its initial position (i.e., $p_i^0 = x_i^0$). The external archive is empty.

Step 2: The fitness value of the particle is calculated on the basis of its current position.

Step 3: The non-dominated solutions are identified based on Pareto dominance and saved to the external archive.

Step 4: The external archive is updated and maintained. Only the non-dominated particles in the external archive are retained. If the number of particles in the external archive exceeds the set capacity, any excess particles are then removed in ascending order based on the niche fitness value until the solution number meets the set capacity.

Step 5: The termination condition is assessed, and the procedure is stopped and the calculation results are output if the iteration τ is equal to T (the maximum number of iteration times). Otherwise, $\tau \leftarrow \tau + 1$.

Step 6: The global optimal position p_g^τ and individual optimal position p_i^τ are determined. On the basis of the niche fitness values of the particles in the external archive, a particle under the global optimal solution is selected through roulette selection. In regard to the individual optimal position, particle x_i^τ is compared to $p_i^{\tau-1}$, and the non-dominated particle is selected as the individual optimal position p_i^τ of the current generation.

Step 7: The velocity and position of the particles are updated based on Equations (66)-(67) and the process returns to Step 2.

5.3 The Floyd algorithm

The steps of the Floyd algorithm are detailed as follows:

Step 1: According to the scheduling scheme of the emergency fleets established by the first-stage model, the time nodes ($t(m_{(re)a})$) are identified when these emergency fleets face an insufficient floating oil bladders capacity. The time nodes are then arranged in time order as the set of the latest arrival time nodes of the transportation fleets ($T^m = \left\{t_1^m, t_2^m, \cdots, t_\phi^m, \cdots t_\Phi^m\right\}$).

Step 2: The time node to be currently resolved in set T^m is t_ϕ^m, which is the $m_{(re)a}$-th ($m_{(re)a} \geq 1$) time an insufficient floating oil bladder capacity occurs while emergency fleet *re* services demand point *a*. All the transportation fleets that meet Constraint (63) are selected to form a set of candidate transportation fleets RT^*. If $RT^* = \varnothing$, the algorithm proceeds Step 3, while otherwise the algorithm turns to Step 4.

Step 3: The ERRB that meets the time window (i.e., Constraint (59)) is selected as the candidate ERRB responsible for providing the current transportation fleet. If multiple candidate ERRBs occur, following the principle of the minimum operating cost of the transportation fleets, ERRB *b* with the largest number of currently reserved vessels is selected to provide transportation fleet *rt* consisting of a minimum number of vessels that satisfies Constraint (63). The travel time determines the earliest arrival time.

When transportation fleet *rt* arrives at demand point *a*, it replaces the empty floating oil bladders of emergency fleet *re* and stores the fully-loaded floating oil bladders. The position of demand point *a* at t_{ϕ}^{m} is the current waiting point of transportation fleet *rt*. If $\phi = \Phi$, the algorithm proceeds to Step 6, and otherwise, for $\phi \leftarrow \phi + 1$, the algorithm returns to Step 2.

Step 4: A transportation fleet (*rt*) is randomly selected from RT^{*}, which determines that the origin of the shortest path of transportation fleet *rt* is the last waiting point (i.e., node *i*), and the destination (i.e., node *j*) is the position of demand point *a* at t_{ϕ}^{m}. The following path judgment equation is constructed:

$$d_{ioj}^{rt} = d_{io}^{rt} + d_{oj}^{rt}(t_{\phi}^{m}), \quad \forall o \in VE \tag{73}$$

Each node o ($\forall o \in VE$) is successively substituted into Equation (73) for evaluation, and path d_{ioj}^{rt*} with the smallest value is selected among all the d_{ioj}^{rt} values, which is the shortest path for transportation fleet *rt* to transport additional floating oil bladders to the demand point *a* at t_{ϕ}^{m}. If the current path d_{ioj}^{rt*} meets the time window (i.e., Constraint (60)), it is substituted into DRT set and RT^{*} set is updated by removing the corresponding *rt* element (i.e., $RT^{*} \leftarrow RT^{*} / \{rt\}$). If $RT^{*} \neq \varnothing$, Step 4 is repeated, and otherwise, the algorithm proceeds to Step 5.

Step 5: If $DRT = \varnothing$, the algorithm returns to Step 3. Otherwise, the smallest value is selected from DRT as $\hat{D}_{ioj}^{rt*}$ and the corresponding travel time is calculated to determine the earliest arrival time. The decision information related to $\hat{D}_{ioj}^{rt*}$ is regared as part of the scheduling scheme. The DRT set is then cleared for the next determination of the shortest travel distance of each candidate transportation fleet. If $\phi = \Phi$, the algorithm proceeds to Step 6, and otherwise, the algorithm proceeds to Step 2.

Step 6: At $\phi = \Phi$, all transportation fleets still at their last waiting points are allowed to return to their origin ERRBs with fully-loaded floating bladders. All the scheduling processes are then recorded as the supplementary transportation scheme developed for all emergency fleets requiring floating oil bladder replenishment. Finally, the calculation results are output.

5.4 Selection of the ideal solution

The common desire of decision makers is to obtain high responsiveness at a lower response cost, that is, to obtain high cost performance. The Pareto fronts are usually unevenly distributed, which implies that there are diverse rates of change, from which important information similar to cost performance can be mined. On this basis, we adopt an alternative solution based on the cost performance method to select the ideal option for Pareto non-dominated solutions.

(1) Mean variability: this refers to the mean value of the slope of the line between any point (except the endpoint) in the Pareto frontier and its adjacent two points. Let Z_1^s and Z_2^s represent the values of the objective functions corresponding to the non-dominated Pareto solution numbered *s* ($s = 2,3,\cdots,S-1$). Without loss of generality, the points of the Pareto frontier are numbered from small to large according to the value of the cost objective function. The mathematical definition of the mean variability of the Pareto solution numbered *s* for the two objective functions is as follows:

$$k_1^s = \frac{1}{2}\cdot\left(\frac{Z_2^s - Z_2^{s-1}}{Z_1^{s-1} - Z_1^s} + \frac{Z_2^{s+1} - Z_2^s}{Z_1^s - Z_1^{s+1}}\right),\quad s = 2,3,\cdots,S-1 \tag{74}$$

$$k_2^s = \frac{1}{2}\cdot\left(\frac{Z_1^{s-1} - Z_1^s}{Z_2^s - Z_2^{s-1}} + \frac{Z_1^s - Z_1^{s+1}}{Z_2^{s+1} - Z_2^s}\right),\quad s = 2,3,\cdots,S-1 \tag{75}$$

(2) In particular, for the endpoint ($s = 1$ or S), the mean variability of the two objective functions is defined as follows:

$$k_1^1 = \frac{1}{2}\cdot\frac{Z_2^2 - Z_2^1}{Z_1^1 - Z_1^2} \tag{76}$$

$$k_2^1 = \frac{1}{2}\cdot\frac{Z_1^1 - Z_1^2}{Z_2^2 - Z_2^1} \tag{77}$$

$$k_1^S = \frac{1}{2}\cdot\frac{Z_2^S - Z_2^{S-1}}{Z_1^{S-1} - Z_1^S} \tag{78}$$

$$k_2^S = \frac{1}{2}\cdot\frac{Z_1^{S-1} - Z_1^S}{Z_2^S - Z_2^{S-1}} \tag{79}$$

(3) Sensitivity ratio: this refers to the ratio of the values of the two kinds of mean variability of a Pareto non-dominated solution in the Pareto frontier to the values of the corresponding objective functions and is defined as follows:

$$\delta_\alpha^s = \frac{k_\alpha^s}{Z_\alpha^s},\quad s = 1,2,\cdots,S,\quad Z_1^s \neq 0,\quad \forall\alpha \in \{1,2\} \tag{80}$$

(4) The above definition shows that the value of the sensitivity ratio reflects the sensitivity of the mean variability of the objective function value relative to the unit value of the objective function. To facilitate the next comparison, the sensitivity ratio must be standardized as follows:

$$\varepsilon_\alpha^s = \frac{\delta_\alpha^s}{\sum_{s=1}^{S}\delta_\alpha^s},\quad s = 1,2,\cdots,S,\quad \forall\alpha \in \{1,2\} \tag{81}$$

(5) Pareto dominance based on sensitivity ratio: similar to the definition of Pareto dominance, if the sensitivity ratios of solution x_i are at least equal to those of x_j, and better than those of x_j in at least one sensitivity ratio, then solution x_i dominates solution x_j (denoted $x_i \succ x_j$). In formal terms, $x_i \succ x_j$ can be defined as follows:

$$(\forall\alpha \in \{1,2\}, i, j \in \{1,2,\cdots,S\},\ \varepsilon_\alpha^i \geq \varepsilon_\alpha^j) \wedge (\exists\alpha \in \{1,2\}, i, j \in \{1,2,\cdots,S\}, \varepsilon_\alpha^i > \varepsilon_\alpha^j) \tag{82}$$

(6) Skewness based on sensitivity ratio: this reflects the degree of preference for different objectives, and its value range is between 0 and 1. w_1^s and w_2^s are the skewness of the Pareto non-dominated solution numbered *s* based on the sensitivity ratio to the objective functions Z_1 and Z_2, respectively, which can be formulated as follows:

$$w_\alpha^s = \frac{\varepsilon_\alpha^s}{\varepsilon_1^s + \varepsilon_2^s},\quad s \in S^*,\quad \forall\alpha \in \{1,2\} \tag{83}$$

where S^* is the set of Pareto non-dominated solutions based on the sensitivity ratio.

When w_1^s is the largest, the corresponding solution is the strongly biased one toward the objective function Z_1, and vice versa. Therefore, the cost performance

method is able to provide decision makers with more convenient quantitative indexes for weighing and comparing, which effectively avoids the subjectivity of the weight coefficient setting.

6 Application of the proposed methodology

6.1 Test instances

During the ConocoPhillips oil spill in the Bohai Bay, over 7,000 barrels of oil and 3,000 barrels of mineral oil-based drilling muds were released into the sea, which polluted an area of approximately 6,200 square kilometers around and northwest of the oilfield. This was one of the largest oil spills in maritime transportation over the past decade. To verify that the proposed model and approaches effectively support such a large-scale oil spill, the test instances are defined based on the ConocoPhillips oil spill in the Bohai Bay. The parameters must be determined prior to vessel dispatching, route planning and resource allocation. Because certain oil spill accident data have not yet been released by the government, we manually substitute derived data based on the information provided by the local maritime bureau to validate the proposed model and approaches, which does not yield essentially different results. The corresponding parameters are set as follows.

(1) Demand information. Four hours ($\hat{T}$) passed from the monitoring of the accident area to the beginning of emergency operations. Aircraft aerial reconnaissance revealed a large and dispersed oil film area at sea. According to the characteristics of the oil films in different areas, the analysis of the required resources shows that there are 24 points with thick oil films in need of cleanup, as shown in Fig. 5.

(2) Oil films (the demand points). Two different drift velocities occur in the contaminated area of the sea under the action of two different currents. Some oil films drift to the south by east 42° at a speed of 1.2 knots. The other films drift to the north by west 36° at a speed of 0.8 knots. The relevant information on the quantity, position and drift velocity of the spilled oil at each demand point is listed in Table 1.

(3) Nearby ERRBs and ports. There are four ERRBs near the contaminated area, namely those of Dalian, Yantai, Tianjin and Qinhuangdao. Moreover, there are four ports nearby, namely, those of Penglai, Longkou, Dongying and Jingtang. The information related to the locations of these ERRBs and ports and the vessel configuration of each ERRB are summarized in Table 2.

(4) Vessels. To simplify the analysis, all vessels are assumed to be of the same type and exhibit the same performance, the details of which are provided in Table 3. In regard to the emergency response, six emergency fleets are expected to be dispatched to service all the demand points.

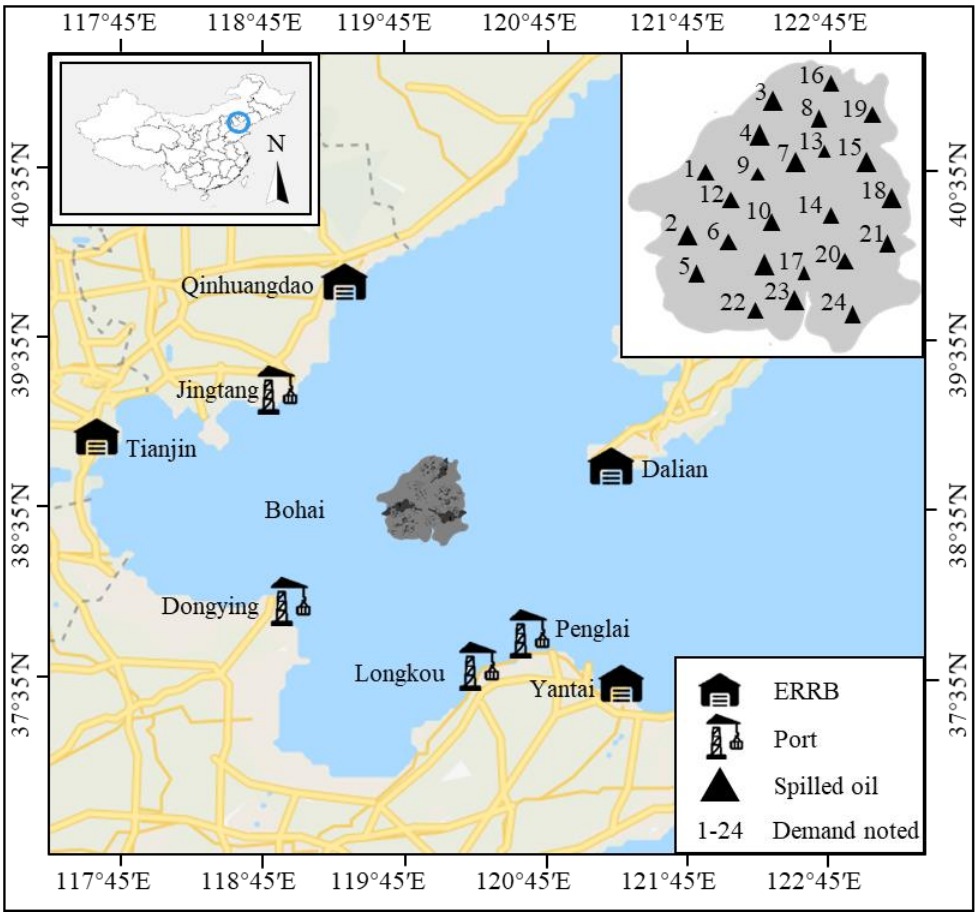

Fig. 5. Distribution of the demand points.

Table 1

Data on the oil films at the demand points.

No.	Oil Quantity (t)	Coordinates (E/N)	Velocity (knots)	No.	Oil Quantity (t)	Coordinates (E/N)	Velocity (knots)
1	50	119.8887 /38.8055	0.8	13	36	119.7528 /38.4276	1.2
2	126	119.6075 /38.5593	0.8	14	64	119.8988 /38.5618	1.2
3	148	119.8108 /38.7249	1.2	15	162	120.0174 /38.6533	1.2
4	40	119.5685 /38.4067	1.2	16	58	120.113 /38.7488	1.2
5	98	119.6444 /38.4683	0.8	17	35	119.8445 /38.4773	0.8
6	67	119.7171 /38.525	0.8	18	153	119.997 /38.5847	1.2
7	154	119.8467 /38.6379	1.2	19	62	119.7234 /38.3042	1.2
8	78	119.8886 /38.6906	1.2	20	52	119.8089 /38.3948	0.8

9	58	119.9925 /38.7771	0.8	21	73	119.9738 /38.522	1.2
10	72	119.7953 /38.5469	0.8	22	93	120.1368 /38.6434	0.8
11	113	119.9666 /38.7054	0.8	23	118	119.9294 /38.3773	0.8
12	45	120.0991 /38.812	1.2	24	69	120.0979 /38.5697	0.8

Table 2
Data on the candidate nearby ERRBs and ports.

No.	Type of nodes	Name of the nodes	Coordinates (E/N)	Number of reserved vessels
25	ERRB	Dalian	121.1333 /38.75	58
26	ERRB	Yantai	121.396 /37.548	62
27	ERRB	Tianjin	117.720833 /38.984722	55
28	ERRB	Qinhuangdao	119.607222 /39.906667	52
29	Port	Penglai	120.67531 /37.81459	-
30	Port	Longkou	120.302275 /37.637814	-
31	Port	Dongying	118.9225 /38.0694	-
32	Port	Jingtang	119.00268 /39.20983	-

Table 3
Data on the emergency and transportation vessels.

Type of vessel	Speed (knots)	Capacity of the bladder (m^3)	Recycling rate (m^3/h)	Cleanup rate (m^2/h)	Operation cost of a self-owned vessel (CNY)	Operation cost of vessel lease (CNY)	Unit travel cost (CNY/n mile)
Emergency vessel	12	400	120	4800	3500	5000	20
Transportation vessel	12	800	-	-	3500	5000	20

6.2 Performance analysis

We utilize MATLAB 2016b to solve the model and follow the proposed HHA proposed. All the numerical experiments are carried out on the same computer with 3.6 GHz i3-9100F processor, 8 GB of RAM, and a 64-bit Microsoft Windows 10 ultimate operating system. With the considerable research data, the appropriate values of all control variables are empirically determined as follows: $N = 50$, $\omega_{\max} = 0.9$, $\omega_{\min} = 0.4$, $c_1 = c_2 = 1.49445$, T = 300, and $\delta_{share} = 3.2$. To investigate the performance of the HHA, it is necessary to compare it to the Non-dominated Sorting Genetic Algorithm II (NSGA-II), which is one of the most appropriate heuristic algorithms for solving resource planning problems and extensively utilized to solve multi-objective models (Abdolhamid et al., 2020). Similarly, the number of chromosomes in the population is set to 50, and the maximum number of iterations is set to 300. The crossover rate is set to 0.9. The mutation rate is set to 0.1.

Since the problem to be resolved is an NP-hard problem, to determine the approximate Pareto optimal solutions of the model, ten runs are performed for each test instance with the HHA and NSGA-II. The sets of approximate Pareto optimal solutions under this specific accident scenario are shown in Fig. 6. It is directly observed that the Pareto solutions obtained with the HAA algorithm generally dominate those obtained with the NSGA-II.

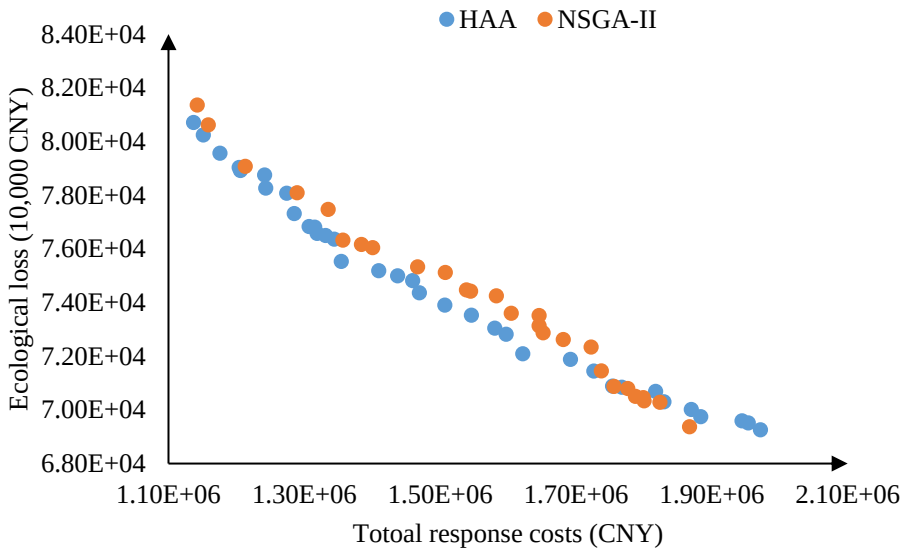

Fig. 6. Computational results of the specific accident scenario.

To further investigate the performance of the two algorithms, three commonly used metrics are adopted as follows: space metric (Ghasemi et al., 2019), mean ideal distance (Ghasemi et al., 2019) and quantity metric (Rezaei et al., 2020). The comparison results in terms of space metric (SM), mean ideal distance (MID), quantity metric (QM) and computation time (CPU) are shown in Table 4. The last row in the table shows the average (Avg) of the values for these four metrics in the ten replications. SM measures the uniformity of the spread of the non-dominated solutions. The smaller the value of SM is, the lower the dispersion of the non-dominated solutions will be. As for MID, it is one of the all-purpose metrics to evaluate convergence of the Pareto-based multi-objective optimization algorithm. The algorithm with a smaller value of MID has a better performance in convergence. In addition, the value of QM is

represented by the number of the obtained non-dominated solutions. Obviously, the larger the value of QM is, the higher quality non-dominated solutions the algorithm can provide for decision makers. According to Table 4, it can be demonstrated that the HHA has better performance in solving the proposed model due to the smaller values of SM and MID and the large value of QM, which implies that the introduction of the niche sharing mechanism can provide more opportunities for the HHA to explore the unexplored feasible region so as to ensure the diversity and robustness of the results. In addition, due to the advantages of simplicity of the heuristic framework of PSO, the HHA can effectively avoid complex genetic operations like selection, crossover and mutation, and performs better than the NSGA-II in computation time.

Table 4
Results of the performance metrics for the case study

No.	HHA				NSGA-II			
	SM	MID	QM	CPU(s)	SM	MID	QM	CPU(s)
1	0.185	0.636	37	339.21	0.191	0.812	29	321.66
2	0.213	0.731	31	327.29	0.285	0.975	30	381.88
3	0.279	0.895	38	327.65	0.200	1.023	29	373.59
4	0.201	0.774	32	343.57	0.254	1.089	27	381.90
5	0.200	0.817	39	351.26	0.265	0.979	29	329.80
6	0.288	0.848	34	333.91	0.180	0.772	28	353.52
7	0.186	0.803	33	327.95	0.248	0.723	33	337.00
8	0.199	0.796	38	330.11	0.180	0.772	28	328.00
9	0.185	0.728	32	332.51	0.265	0.711	29	350.73
0	0.185	0.767	39	337.68	0.295	0.682	31	366.17
Avg	0.212	0.779	35.30	335.11	0.237	0.854	29.30	352.42

6.3 Application results

Similar to previous studies of most multi-objective optimization problems, the non-dominated solutions obtained do not directly provide decision-makers with a specific scheduling scheme. To furnish the decision makers with high-quality decision support, we adopt the cost performance method proposed above to determine the ideal option in the set of non-dominated solutions. First, the solutions in the Pareto frontier are numbered in ascending order of the total response cost. Without loss of generality, we set $\alpha = 1$ as the serial number of the responsiveness objective, while $\alpha = 2$ is set for that of the cost objective. Following the procedure of the cost performance method proposed in Section 5.4, we obtain the corresponding mean variability k_α ($\forall \alpha \in \{1,2\}$), sensitivity ratio δ_α ($\forall \alpha \in \{1,2\}$) and standardized sensitivity ratio ε_α ($\forall \alpha \in \{1,2\}$), the details of which are summarized in Table 5. Fig. 7 shows the distribution of the sensitivity ratio after standardization and Fig. 8 shows the distribution of the Pareto frontier based on the standardized sensitivity ratio.

Table 5
Corresponding parameters of the cost performance method.

No	$k_1(\times 10^2)$	$k_2(\times 10^{-2})$	$\delta_1(\times 10^{-3})$	$\delta_2(\times 10^{-8})$	$\varepsilon_1(\times 10^{-2})$	$\varepsilon_2(\times 10^{-2})$

1	0.311	3.213	0.386	2.825	0.615	3.673
2	0.336	2.996	0.418	2.602	0.667	3.382
3	0.447	2.327	0.561	1.979	0.895	2.572
4	0.349	3.975	0.442	3.301	0.704	4.291
5	1.143	3.273	1.448	2.714	2.309	3.528
6	1.078	15.157	1.368	12.206	2.181	15.867
7	0.821	15.232	1.049	12.251	1.672	15.925
8	0.878	3.693	1.125	2.898	1.793	3.767
9	0.300	4.486	0.388	3.490	0.619	4.537
10	2.280	1.226	2.968	0.938	4.731	1.219
11	2.129	3.466	2.772	2.634	4.418	3.424
12	0.881	3.654	1.150	2.770	1.833	3.601
13	1.264	0.855	1.653	0.642	2.635	0.835
14	0.521	4.533	0.683	3.372	1.088	4.384
15	0.869	4.298	1.151	3.173	1.834	4.125
16	1.519	0.661	2.020	0.469	3.220	0.609
17	1.334	0.753	1.779	0.524	2.836	0.681
18	0.730	2.703	0.976	1.851	1.556	2.407
19	0.516	2.914	0.695	1.983	1.107	2.577
20	0.931	1.091	1.260	0.724	2.008	0.941
21	0.882	1.174	1.200	0.759	1.912	0.987
22	0.722	1.385	0.988	0.876	1.576	1.139
23	0.533	2.164	0.731	1.355	1.166	1.761
24	1.830	1.626	2.538	1.002	4.045	1.303
25	2.057	0.780	2.862	0.461	4.562	0.599
26	0.640	1.658	0.896	0.960	1.429	1.248
27	1.939	1.176	2.736	0.671	4.360	0.872
28	3.305	0.303	4.666	0.171	7.437	0.223
29	1.767	1.738	2.500	0.957	3.985	1.243
30	0.865	1.937	1.230	1.059	1.961	1.376
31	0.962	1.334	1.374	0.713	2.190	0.927
32	2.267	1.105	3.250	0.586	5.181	0.762
33	2.616	0.538	3.759	0.277	5.992	0.360
34	0.952	1.133	1.369	0.580	2.183	0.754
35	1.243	0.998	1.795	0.506	2.860	0.658
36	2.479	0.437	3.586	0.219	5.715	0.285
37	1.736	1.798	2.521	0.864	4.019	1.122
38	0.305	3.280	0.446	1.565	0.711	2.034

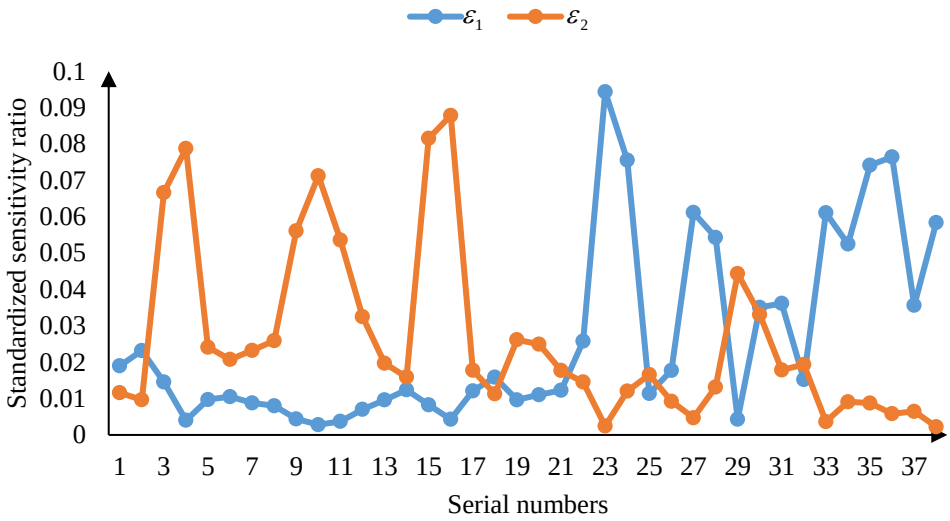

Fig. 7. Sensitivity ratio distribution after standardization.

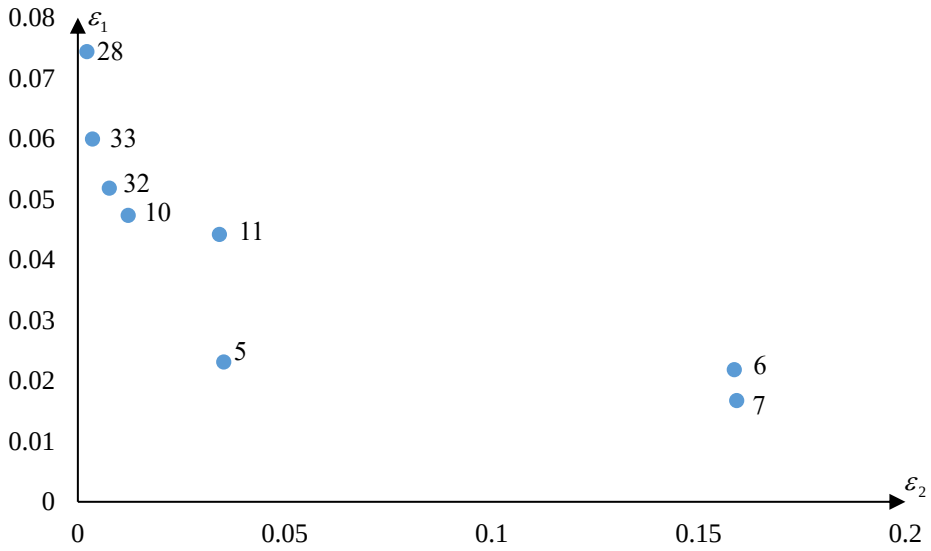

Fig. 8. the Pareto frontier based on the standardized sensitivity ratio.

In the original Pareto solution set, there are 30 solutions that are filtered out according to the Pareto dominance of the sensitivity ratio as described in Section 5.4. The 8 retained solutions constitute a subset of Pareto non-dominated solutions based on the standardized sensitivity ratio, which further narrows the range of ideal options for decision makers. In emergency management, for the sake of humanitarianism, decision makers usually prefer the responsiveness objective over the cost objective. When both the values of the responsiveness and cost objectives are acceptable, the solution with the largest skewness to the responsiveness objective is supposed to be selected as the most suitable option. Therefore, the solution numbered 28 is selected as the ideal solution, the skewness of which to the responsiveness objective is 0.971, which is the largest value. The corresponding scheduling scheme is listed in Tables 6 and 7. Under such a scheme, the value of the ecological loss is 7.08×10^{8} CNY, and the total response cost amounts to 1.77×10^{6} CNY. Table 8 indicates the latest time allowed for the supplementary resources and the earliest arrival time of the actual transportation fleet under the scheduling scheme skewed toward responsiveness. When the decision-

making environment is a under severe budgetary pressure, decision makers may choose the solution numbered 7, the skewness of which to the cost objective reaches 0.905. The corresponding scheduling scheme is listed in Tables 9 and 10. Under this scheme, the value of the ecological loss is 7.83×10^{8} CNY, and the total response cost amounts to 1.24×10^{6} CNY. Table 11 describes the situation of the transportation timeframe of the supplementary resources under the scheduling scheme skewed toward the total response cost.

Table 6
Scheduling scheme of the emergency fleets skewed toward responsiveness.

No. of emergency fleets	Subordinate to	Route planning	Number of vessels	Area of cleanup (m^2)
1	Dalian	25-18-13-25	28	8.20×10^{5}
2	Dalian	25-3-7-9-21-11-6-25	30	3.04×10^{6}
3	Yantai	26-4-10-12-5-23-26	28	1.99×10^{6}
4	Dalian	25-2-15-8-19-1-25	28	2.38×10^{6}
5	Dalian	25-16-17-20-24-25	24	1.14×10^{6}
6	Dalian	25-22-14-25	28	7.53×10^{5}

Table 7
Scheduling scheme of the transportation fleets skewed toward responsiveness.

No. of transportation fleets	Subordinate to	Number of vessels	Route planning
1	Qinhuangdao	14	28-18-29-15-29-19-28
2	Qinhuangdao	15	28-3-32-9-32-23-32-11-28
3	Tianjin	12	27-17-27
4	Tianjin	14	27-2-32-5-27
5	Yantai	14	26-14-29-8-26
6	Tianjin	15	27-7-29-21-32-6-27
7	Qinhuangdao	14	28-10-32-5-32-1-28
8	Yantai	12	26-20-26

Table 8
Transportation timeframe of the supplementary resources under the scheduling scheme skewed toward responsiveness.

No. of demand points	Latest arrival time (h)	Earliest arrival time (h)	No. of demand points	Latest arrival time (h)	Earliest arrival time (h)
18	7.63	7.45	8	19.03	18.12
3	8.18	6.64	5	19.63	16.26
17	8.99	8.19	19	22.68	21.99
2	9.45	7.34	5	22.96	18.94
14	10.89	6.70	21	25.87	18.01
7	12.02	9.48	23	26.95	24.32
10	12.25	6.15	1	30.93	27.98

20	12.61	8.42	11	34.39	32.69
15	15.40	15.08	6	38.02	35.46
9	18.02	15.98			

Table 9
Scheduling scheme of the emergency fleets skewed toward the total response cost.

No. of emergency fleets	Subordinate to	Route planning	Number of vessels	Area of cleanup (m^2)
1	Tianjin	27-17-6-24-27	16	9.60×10^5
2	Yantai	26-13-5-18-19-26	15	1.92×10^6
3	Yantai	26-2-23-8-21-14-26	16	2.57×10^6
4	Yantai	26-15-9-16-3-12-26	15	2.60×10^6
5	Tianjin	27-22-7-1-11-27	16	2.20×10^6
6	Yantai	26-20-10-4-26	15	9.43×10^5

Table 10
Scheduling scheme of the transportation fleets skewed toward the total response cost.

No. of transportation fleets	Subordinate to	Number of vessels	Route planning
1	Dalian	8	25-15-29-7-29-18-29-16-29-3-25
2	Qinhuangdao	8	28-22-31-24-28
3	Dalian	8	25-20-29-4-29-8-29-21-29-21-29-14-29-14-29-12-25
4	Qinhuangdao	8	28-6-32-9-32-1-32-11-28
5	Dalian	8	25-2-32-23-25
6	Qinhuangdao	8	28-5-28
7	Dalian	8	25-15-29-18-29-8-29-3-25
8	Qinhuangdao	8	28-10-28
9	Dalian	8	25-6-32-9-32-1-32-11-25
10	Tianjin	8	27-2-32-23-27
11	Qinhuangdao	8	28-5-28
12	Dalian	8	25-7-29-7-29-18-29-18-29-19-29-3-29-3-25

Table 11
Transportation timeframe of the supplementary resources under the scheduling scheme skewed toward the total response cost.

No. of demand points	Latest arrival time (h)	Earliest arrival time (h)	No. of demand points	Latest arrival time (h)	Earliest arrival time (h)
15	10.52	4.13	18	27.22	25.39
22	11.23	6.82	8	30.34	28.65
20	11.46	5.29	18	30.55	28.09
6	12.08	6.26	1	31.72	28.57

2	12.37	6.32	16	32.06	31.73
5	12.88	6.49	8	33.68	26.29
15	13.86	3.99	18	33.89	33.73
10	15.28	5.98	1	35.05	25.24
6	15.41	6.14	3	35.83	34.92
2	15.70	7.02	19	37.78	37.06
5	16.21	6.32	21	38.01	36.58
7	16.76	4.26	11	39.06	38.90
24	19.61	18.99	3	39.16	36.39
23	19.85	19.55	21	41.34	39.38
7	20.09	17.77	11	42.39	35.55
4	20.68	20.38	3	42.50	41.07
9	20.69	18.56	14	45.00	42.40
23	23.18	22.46	3	45.83	45.31
7	23.42	23.27	14	48.33	45.87
18	23.89	19.88	12	49.74	49.16
9	24.02	21.46			

The most obvious difference between the two schemes is the size of the fleets. There is no doubt that the fleet size of the scheme biased toward the responsiveness objective is much larger than that of the scheme biased toward the cost objective. In addition, regarding the selection of the ERRBs to provide the emergency fleets, the two schemes also exhibit differences. The responsiveness-oriented scheme tends to select Dalian, which is the closest to the initial position of the contaminated area, to provide emergency fleets to ensure that the emergency service needs of the contaminated area are met as quickly as possible. The cost-oriented scheme assigns relatively far away ERRBs such as Yantai and Tianjin to be responsible for emergency fleets, which is mainly a cost-saving measure. With increasing travel time of the emergency fleets, the latest time allowed for the supplementary resources is postponed, and more time is allowed for the transportation fleets to transport supplies, which is helpful to minimize the number of transportation fleets and the number of temporarily acquired vessels. Interestingly, the transportation fleets tend to exhibit a relatively singular choice of transit points, with few fleets choosing different transit points. In fact, this indicates that there exists a principle of proximity when the transportation fleets select the transport objects of supplies, to ensure a high transportation efficiency, which contributes to the cost objective.

6.4 Sensitivity analysis

We also perform a sensitivity analysis to demonstrate how changes in the parameters of the decision-making environment affect the computational results obtained with the proposed model considering the time-varying conditions. The parameters involved in the analysis include the shipping speed (vk), oil film drift speed (v_a, $a \in A$) and emergency time difference ($\hat{T}$). The reason why these parameters are selected is because any change in the related factors can considerably impacts the values of the objective functions, and the values of these parameters exhibit a wide range of

variation during the response to different accidents according to our interviews with the maritime authority.

6.4.1 Sensitivity to the shipping speed

The impact of the change of shipping speed by -40%, -20% , +20% and +40% on the value of the ecological loss and total response cost is shown in Fig. 9. Both objectives are sensitive to changes in the shipping speed. However, the change in the values of both objective functions is more notable when the shipping speed decreases. This phenomenon most likely occurs due to the irregular pattern of the oil film change. In reality, the diffusion rate of the oil film area does not remain constant but increases with increasing area. With decreasing shipping speed, the emergency fleets take longer to reach the demand points, which provides the oil films with a longer time for fast diffusion, leading to a considerable increase in the demand for emergency services. The increase in demand results in a long cleanup time and high response costs. When dealing with the oil film at the next demand point, this phenomenon is further intensified, similar to the bullwhip effect. Under the influence of a series of chain reactions, a decreasing shipping speed could lead to major changes in both the responsiveness and total response cost.

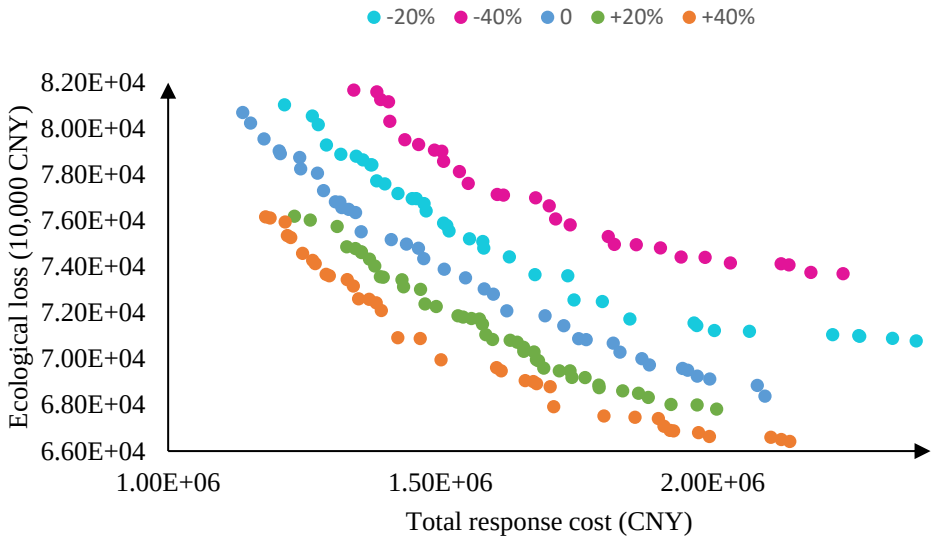

Fig. 9. Impact of the shipping speed change.

6.4.2 Sensitivity to the drift speed

The drift speed of oil films at sea is one of the main uncertain factors during the emergency response. Fig. 10 shows the analysis outcome of the sensitivity of the multi-objective model by investigating the impacts of varying the drift speed by -40%, -20%, +20% and +40%. As shown in the figure, both the responsiveness and cost objectives vary with the drift velocity, but the trend is complex. Generally, with increasing the drift speed, non-dominated solutions move a certain distance toward the origin direction, indicating that the emergency response achieves a better responsiveness at a lower cost. The main reason is that the increase in drift speed shortens the distance between the oil films and the coast for fast emergency services and hence boosts the responsiveness. Moreover, when the transportation fleets transport floating oil bladders to the

emergency fleets, thus providing emergency services to the demand points, the travel time is reduced to a certain extent so that fewer transportation fleets are needed, which decreases the response cost. Notably, this phenomenon gradually decreases or almost disappears with increasing input of emergency resources. This occurs because as the size of the emergency fleet increases, so does the responsiveness of the emergency response and the overall time of the emergency response is considerably reduced. Before major difference in the oil film drift distance between the diverse decision-making environments occurs, the emergency fleets have already completed the provision of emergency services.

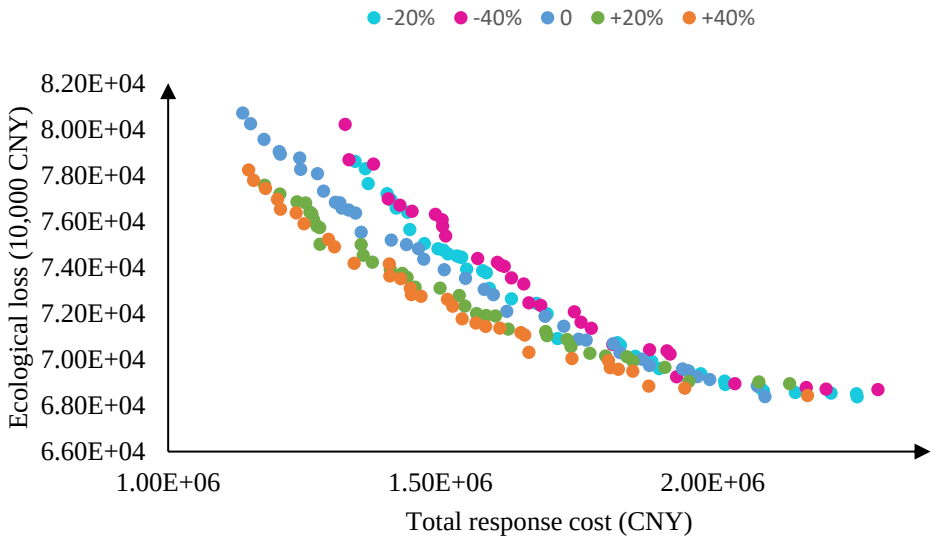

Fig. 10. Impact of the drift speed change.

6.4.3 Sensitivity to the differences in the emergency response time

When a large-scale oil spill accident occurs at sea, the emergency response is not immediately activated. First, the monitoring method is applied to detect the oil spillage area and collect relevant data, and the command center then formulates the emergency scheme according to the actual situation. Hence, a time difference occurs between the completion of contaminated area monitoring and the launch of emergency operations. Fig. 11 shows the impacts of the considered time difference changes of -40%, -20% +20% and +40% on the model objective. It is observed that the distribution of non-dominated solutions in the different decision-making environments is not significantly different at the beginning, but with increasing emergency resources, the gap gradually expands. This is the exact opposite of the phenomenon shown in Fig. 10. The main reason for this occurrence is that the emergency response time differs. When the emergency response cost is low, the responsiveness of the emergency fleets is correspondingly low, and the emergency response time is generally long. Herein, the difference in the demand for emergency services caused by the change in emergency time difference is relatively limited in terms of its proportion of the total demand. Nevertheless, with increasing emergency resources and emergency fleet responsiveness, the oil film diffusion process at all demand points is restrained, thus greatly reducing

the total demand for emergency services. In this case, the difference in the demand for emergency services caused by the change in emergency time difference increases proportionally to the total demand, and the impact of the emergency time difference on the responsiveness becomes more apparent.

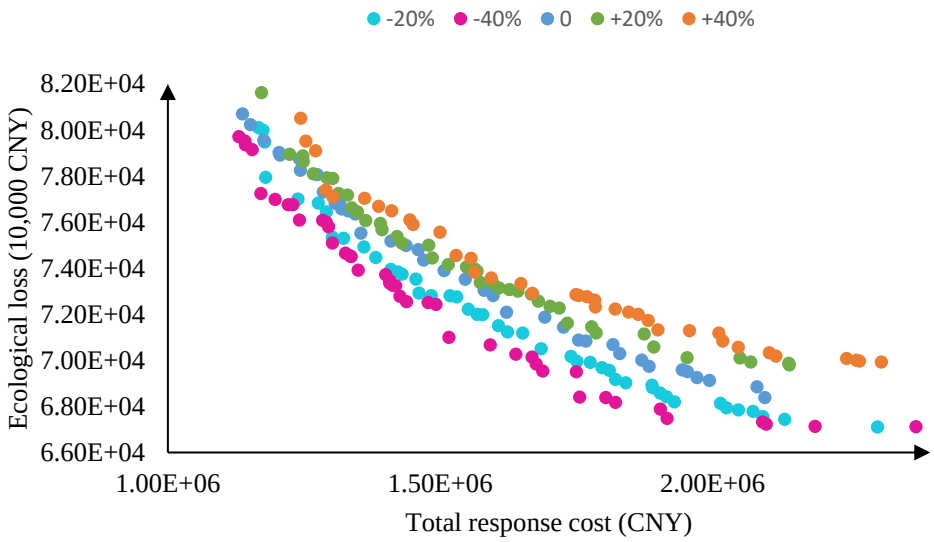

Fig. 11. Impact of the time difference change.

7 Conclusions

In this paper, we propose a dynamic multi-objective location-routing model considering time-varying factors to support the real-world emergency response in a large-scale oil spill accident. To facilitate the solution of the proposed model, it is converted into a two-stage model. In view of the specifics of the two-stage model, we propose the HHA, which combines the IMPSO algorithm with the Floyd algorithm. Considering that the non-dominated solutions obtained by solving multi-objective optimization models do not directly provide decision makers with a specific scheduling scheme, we adopt the cost performance method to help decision makers determine the ideal scheduling scheme. This method effectively avoids the setting of weight coefficients, which often involves a subjective bias. A numerical analysis of a large-scale oil spill accident that occurred in the Bohai Bay is conducted to illustrate the application of the proposed approaches. By comparing the scheduling schemes based on the different preferences of decision makers, it is found that these approaches provide scientific and rational decision support according to the actual decision-making environment, while the findings also verify the effectiveness and feasibility of the proposed model. To further evaluate the performance of the dynamic model with time-varying features for practical implications, we also consider certain randomly generated numerical instances to assess the sensitivity of the objectives with respect to selected critical parameters. The results of the sensitivity analysis demonstrate that both the responsiveness and cost objectives are sensitive to these parameters, but the sensitivity of these objectives varies greatly between the diverse decision-making environments. These changes in sensitivity are closely related to the characteristics of the oil spill

emergency response, which further confirms the practical feasibility of the proposed model and approaches. The above series of quantitative analyses facilitates the investigation of the application of the dynamic multi-objective location-routing model and the HHA to other multi-objective emergency logistics problems with time-varying features.

Although our study bridges several notable gaps between the literature and real accident conditions, a future extension should explore other improvements. To further address the complexity of the oil spill emergency resource scheduling process, in future research, based on analysis of the dynamic motion of oil films, we will examine the emergency logistics problem in more detail. First, after a major oil spill accident, the vastness of the polluted area produces varying oil film conditions at distinct demand points that necessitate different cleanup stages, leading to differences in emergency resource requirements. However, we have only proposed a mono-resource optimization model for the response to oil spills. Second, since no material storage conditions are available at sea, various resources are only delivered in stages to the demand points according to the emergency response disposal schedule. The scheduling coordination of different emergency resources remains to be resolved. Finally, compatibility issues persist between the different resources and transportation mean. In particular, distinct modes of transportation are applicable to different resources. This paper has only considered emergency vessels participating in oil spill emergency, but has not yet analyzed the coordinated transportation of emergency resources by both sea and air.

Reference

Abdolhamid, Z., Mehrdad, K., Ali, H.K., (2020). Multi-objective decision-making model for distribution planning of goods and routing of vehicles in emergency multi-objective decision-making model for distribution planning of goods and routing of vehicles in emergency. International Journal of Disaster Risk Reduction, 48, 101587.

Ahmadi, M., Seifi, A., Tootooni, B., (2015). A humanitarian logistics model for disaster relief operation considering network failure and standard relief time: A case study on San Francisco district. Transp. Res. Part E: Logist, Transp. rev. 75, 145-163.

Alem, D., Clark, A., Moreno, A., (2016). Stochastic network models for logistics planning in disaster relief. Eur. J. Oper. Res, 255(1), 187-206.

Ando, A.W., Khanna, M., Amy, wildermuth, et al., (2004). Natural resource damage assessment: methods and cases. Illinois: Illinois waste management and research center，25.

Baharmand, H., Comes, T., Lauras, M., (2020). Supporting group decision makers to locate temporary relief distribution centres after sudden-onset disasters: A case study of the 2015 Nepal earthquake. International Journal of Disaster Risk Reduction, 45, 101455.

Baharmand, H., Comes, T., Lauras, M., (2019). Bi-objective multi-layer location–allocation model for the immediate aftermath of sudden-onset disasters. Transp. Res. Part E: Logist. Transp. Rev, 127(1), 86-110.

Chakravarty, A.K., (2014). Humanitarian relief chain: rapid response under uncertainty.

Int. J. Prod. Econ, 151, 146–157.

Campbell, L., Clarke, P.K., (2018). Making operational decisions in humanitarian response. Technical Report Active Learning Network for Accountability and Performance in Humanitarian Action (ALNAP).

Cao, C.J., Li, C.D., Yang, Q., Liu, Y., Qu, T., (2018). A novel multi-objective programming model of relief distribution for sustainable disaster supply chain in large-scale natural disasters. J. Cleaner Prod, 174: 1422-1435.

Charles, A., Lauras, M., Van Wassenhove, L.N., Dupont, L., (2016). Designing an efficient humanitarian supply network. J. Oper. Manage, 47, 58 – 70.

Chen, X., Liu, L., Huang, W., (2016). The detection and prediction for oil spill on the sea based on the infrared images. Infrared Physics & Technology, 77, 391-404.

Daniel, R.R., Gina, G., Ruben, Y.P., (2020). Planning the delivery of relief supplies upon the occurrence of a natural disaster while considering the assembly process of the relief kits. Socio-Economic Planning Sciences, 69, 100682.

Dror, M., Trudeau, P., (1989). Savings by split delivery routing. Transp. Sci, 23, 141–145.

Fay, J.A., (1979). Physics Processes in the Spread of Oil on a Water Surface. Proceedings of the Joint Conference on Prevention and Control of Oil Spills, 463-467.

Feng, J.R., Gai, W.M., Li, J.Y., (2019). Multi-objective optimization of rescue station selection for emergency logistics management. Safety Science, 120, 276-282.

Garrett, R.A., Sharkey, T.C., Grabowski, M., et al., (2017). Dynamic resource allocation to support oil spill response planning for energy exploration in the Arctic. European Journal of Operational Research, 257, 272-286.

Ghasemi, P., Khalili-Damghani, P., Hafezalkotob, A., et al., 2019. Uncertain multi-objective multi-commodity multi-period multi-vehicle location-allocation model for earthquake evacuation planning. Applied Mathematics and Computation, 350, 105-132.

Gill, D.A., Ritchie, L.A., Picou, J.S., (2016). Sociocultural and psychosocial impacts of the exxon valdez oil spill: Twenty-four years of research in Cordova, Alaska. Extract. Ind. Soc, 3(4), 1105-1116.

Gökalp, E., Ümit, B., (2020). A robust disaster preparedness model for effective and fair disaster response. European Journal of Operational Research, 280(2): 479-494.

Gralla, E., Goentzel, J., Fine, C., (2016). Problem formulation and solution mechanisms: a behavioral study of humanitarian transportation planning. Prod. Oper. Manage, 25, 22–35.

Grubesic, T.H, Nelsona, J.R., Wei, R., (2019). A strategic planning approach for protecting environmentally sensitive coastlines from oil spills: Allocating response resources on a limited budget. Marine Policy, 108, 103549.

He, S., Gu, F., Li, J.P., (2013). Emergency command of China's international petroleum cooperative emergencies: take oil spill incident of Bohai Bay as an example. Ecological Economy, 2, 373-376.

Hoyos, M.C., Morales, R.S., Akhavan-Tabatabaei, R., (2015). Or models with

stochastic components in disaster operations management: a literature survey. Comput. Ind. Eng, 82, 183–197.

Hu, C., Liu, X., Hua, Y., (2016). A bi-objective robust model for emergency resource allocation under uncertainty. Int. J. Prod. Res, 54, 7421–7438.

Hu S.L., Han C.F, Dong Z.S., Meng L.P., (2019). A multi-stage stochastic programming model for relief distribution considering the state of road network. Transportation Research Part B: Methodological, 123, 64-87.

Huang, K., Jiang, Y., Yuan, Y., Zhao, L., (2015). Modeling multiple humanitarian objectives in emergency response to large-scale disasters. Transp. Res. Part E: Logist. Transp. Rev, 75, 1–17.

Huang, X.L., Ren, Y.T., Zhang, J.A., et al., (2020). Dynamic Scheduling Optimization of Marine Oil Spill Emergency Resource. Journal of Coastal Research,107, 437-442.

ITOPF, (2020). Statistics - ITOPF. http://www.itopf.com/knowledge-resources/data-statistics/statistics/.

Jomon, A.P., Wang, X.F., (2019). Robust location-allocation network design for earthquake preparedness. Transportation Research Part B: Methodological, 119, 139-155.

Kowalski-Trakofler, K.M., Vaught, C., Scharf, T., (2003). Judgment and decision making under stress: an overview for emergency managers. Int. J. Emergency Manage, 1, 278–289.

Kunz, N., Van Wassenhove, L.N., Besiou, M., Hambye, C., Kovács, G., (2017). Relevance of humanitarian logistics research: best practices and way forward. Int. J. Oper. Prod. Manage, 37(11), 1585-1599.

Li, L., Wang, B., Wang, A.J., (2014a). An emergency resource allocation model for maritime chemical spill accidents. Journal of Management Analytics, 1(2), 146-155.

Li, P., Cai, Q., Lin, W., Chen, B., Zhang, B., (2016). Offshore oil spill response practices and emerging challenges. Mar. Pollut. Bull, 110 (1), 6–27.

Li P., Chen B., Zhang B., et al., (2014b). Monte Carlo simulation-based dynamic mixed integer nonlinear programming for supporting oil recovery and devices allocation during offshore oil spill responses. Ocean & Coastal Management, 89(2), 58–70.

Lin Y.H., Batta R., Rogerson P.A., et al., (2011). A logistics model for emergency supply of critical items in the aftermath of a disaster. Socio-Economic Planning Sciences, 45(4), 132-145.

Liu, J., Guo, L., Jiang, J.P., et al. (2018), Emergency material allocation with time-varying supply-demand based on dynamic optimization method for river chemical spills. Environment Science and Pollution Research, 25,17343-17353.

Liu, S.K., Leendertse J.J., (1981). A 3-D oil spill model with and without ice cover. Proceedings of the International Symposium on Mechanics of Oil Slicks. Proceedings of the International Symposium on Mechanics of Oil Slicks． Paris， France: Rand Corp.

Liu, Y.J., Lei, H.T., Wu, Z.Y., Zhang, D.Z., (2019). A robust model predictive control

approach for post-disaster relief distribution. Computers & Industrial Engineering, 135, 1253-1270.

Loree, N., Aros-Vera, F., (2018). Points of distribution location and inventory management model for post-disaster humanitarian logistics. Transp. Res. Part E: Logist. Transp. Rev, 116, 1–24.

Lu, C.C., Ying, et al., (2016). Real-time relief distribution in the aftermath of disasters – A rolling horizon approach. Transportation Res. Part E Logistics Transportation Rev, 93, 1–20.

Maharjan, R., Hanaokab S., (2020). A credibility-based multi-objective temporary logistics hub location-allocation model for relief supply and distribution under uncertainty. Socio-Economic Planning Sciences, 70, 100727.

Mehmet, K.O., Sule, I.S., (2020). A two-stage stochastic model for location planning of temporary medical centers for disaster response. International Journal of Disaster Risk Reduction, 44, 101426.

Mete, H.O., Zabinsky, Z.B., (2010). Stochastic optimization of medical supply location and distribution in disaster management. Int. J. Prod. Econ, 126, 76 – 84.

Moreno, A., Alem, D., Ferreira, D., Clark A., (2018). An effective two-stage stochastic multi-trip location-transportation model with social concerns in relief supply chains. European Journal of Operational Research, 269, 1050-1071.

Najafi, M., Eshghi, K., Dullaert, W., (2013). A multi-objective robust optimization model for logistics planning in the earthquake response phase. Transport. Res. Part E: Logist. Transport. Rev, 49, 217 – 249.

Oscar, R.E., Pavel A., Christopher, B., (2018). Dynamic formulation for humanitarian response operations incorporating multiple organisations. International Journal of Production Economics, 204, 83-98.

Payam A.H., Mohammad R., 2019. Response planning for accidental oil spills in Persian Gulf: A decision support system (DSS) based on consequence modeling. Marine Pollution Bulletin, 140:116-128.

Ransikarbum K., Masson S.J., (2014). Multiple-objective analysis of integrated relief supply and network restoration in humanitarian logistics operations. International Journal of Production Research, 54 (1), 49–68.

Ransikarbum, K., Mason, S.J., (2016). Goal programming-based post-disaster decision making for integrated relief distribution and early-stage network restoration. Int.J. Prod. Econ, 182, 324 – 341.

Rezaei, M., Afsahi, M., Shafiee, M., et al., 2020. A bi-objective optimization framework for designing an effcient fuel supply chain network in post-earthquakes. Computers & Industrial Engineering, 147, 106654.

Sabbaghtorkan, M., Batta, R,, He, Q., (2020). Prepositioning of assets and supplies in disaster operations management: Review and research gap identification. European Journal of Operational Research, 284, 1-19.

U.S. National Commission on the Deepwater Horizon Oil Spill and Offshore Drilling, (2011). Deep Water—The Gulf Oil Disaster and the Future of Offshore Drilling. Report

to the President. U.S. National Commission on the Deepwater Horizon Oil Spill and Offshore Drilling, USA, p. 398.

Wang, H., Du, L., Ma, S., (2014). Multi-objective open location-routing model with split delivery for optimized relief distribution in post-earthquake. Transportation Research Part E: Logistics and Transportation Review, 69:160-179.

Wang, Y., Liu, X., Yu, X., et al., (2018). Assessing response capabilities for responding to ship-related oil spills in the Chinese Bohai Sea. International Journal of Disaster Risk Reduction, S2212420918302668.

Wang, Y.J., Lee, K., Liu, D.Y., et al., (2020). Environmental impact and recovery of the Bohai Sea following the 2011 oil spill. Environmental Pollution, 263: 114343.

Ye, X.D., Chen, B., Li, P., et al., (2019). A simulation-based multi-agent particle swarm optimization approach for supporting dynamic decision making in marine oil spill responses. Ocean and Coastal Management, 172, 128-136.

Yin, J., (2019). Analysis and reflection on causation and emergency disposal of Sanchi crash-blasting accident. Navigation of China, 42(1), 42-46.

Xiong, S.A., Long, H.L., Tang, G.P., et al., (2015). The management in response to marine oil spill from ships in China: A systematic review. Marine Pollution Bulletin, 96, 7-17.

Xu, S., Xu, Z., Liu, Y., (2016). Optimal dispatch of oil spill resources considering resource priority. IEEE International Conference on Intelligent Transportation Engineering, DOI: 10.1109/ICITE.2016.7581311.

Zhang, J., Liu, H., Yu, G., et al., (2019). A three-stage and multi-objective stochastic programming model to improve the sustainable rescue ability by considering secondary disasters in emergency logistics. Computers & Industrial Engineering, 135, 1145-1154.

Zhang, R., Chang, P.C., Song, S., Wu, C., (2017). Local search enhanced multi-objective PSO algorithm for scheduling textile production processes with environmental considerations. Appl. Soft Comput. J, 61, 447e467.

Zhao, Y., Wu, G., Gui, F., et al., (2019). Optimal Coordination Path Selecting Method for Conduction Transformation Based on Floyd Algorithm. Procedia Computer Science, 162, 227-234.

Zhou Y., Liu J., Zhang Y., et al., (2017). A multi-objective evolutionary algorithm for multi-period dynamic emergency resource scheduling problems. Transportation Research Part E Logistics & Transportation Review, 99:77-95.